New Fluorescent Porphyrins with High Two-Photon Absorption Cross-Sections Designed for Oxygen-Sensitization: Impact of Changing the Connectors in the Peripheral Arms

Limiao Shi [1], Zhipeng Sun [1], Nicolas Richy [1], Olivier Mongin [1], Mireille Blanchard-Desce [2], Frédéric Paul [1] and Christine O. Paul-Roth [1,*]

[1] Univ. Rennes, INSA Rennes, CNRS, Institut des Sciences Chimiques de Rennes (ISCR)—UMR 6226, F-35000 Rennes, France; lmshi09@yahoo.com (L.S.); sunzpciomp@126.com (Z.S.); nicolas.richy@univ-rennes1.fr (N.R.); olivier.mongin@univ-rennes1.fr (O.M.); frederic.paul@univ-rennes1.fr (F.P.)

[2] Univ. Bordeaux, Institut des Sciences Moléculaires, CNRS UMR 5255), 351 Cours de la Libération, 33405 Talence, France; mireille.blanchard-desce@u-bordeaux.fr

* Correspondence: christine.paul@univ-rennes1.fr or christine.paul@insa-rennes.fr; Tel.: +33-02-2323-6372

Contents

1. Retrosynthetic analysis and synthesis of key precursors for the starting aldehydes
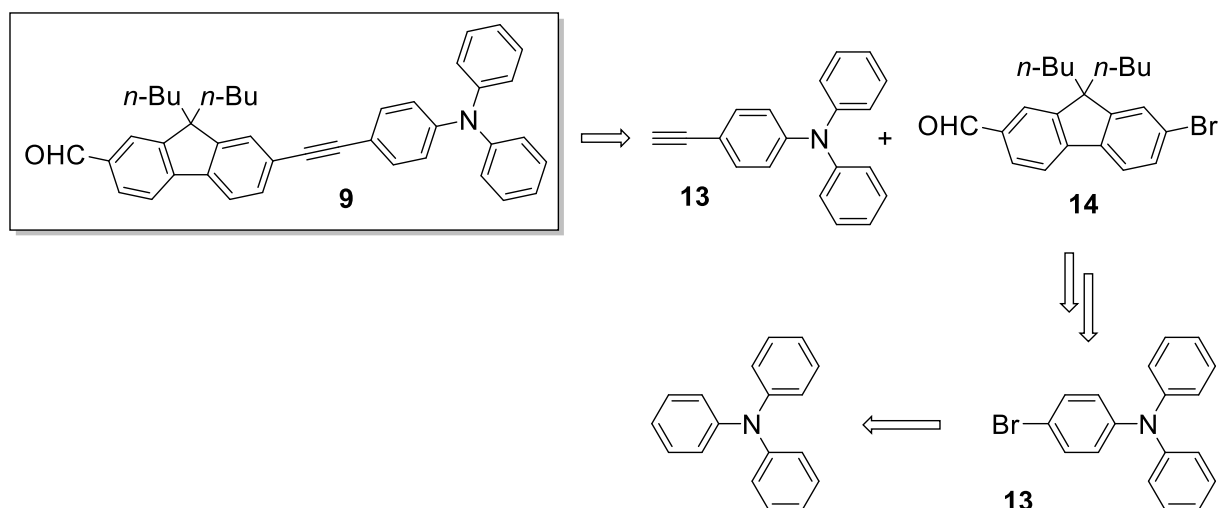
A/ Fluorenylaldehyde 9

Figure S1. Retrosynthetic analysis of fluorenylaldehyde **9** with a diphenylamine endgroup.

Synthesis of 4-ethynyl-*N,N*-diphenylaniline 13. Compound **13** was obtained in three steps from commercial triphenylamine (Figure S1). In detail, bromination of triphenylamine provided monobromo-compound **a**[28] which was obtained pure after recrystallization from ethanol (71% yield). The protected alkyne **b**[29] was synthesized in 61% yield by Sonogashira reaction coupling[30] of **a** with ethynyltrimethylsilane. Then alkyne **b,** with subsequent cleavage of the TMS group, provides access to the terminal alkyne **13**[29] in 98% yield. We can note that when this reaction time is prolonged, the yield improves because this reaction is slowed down by the electron-rich nature of triphenylamine.
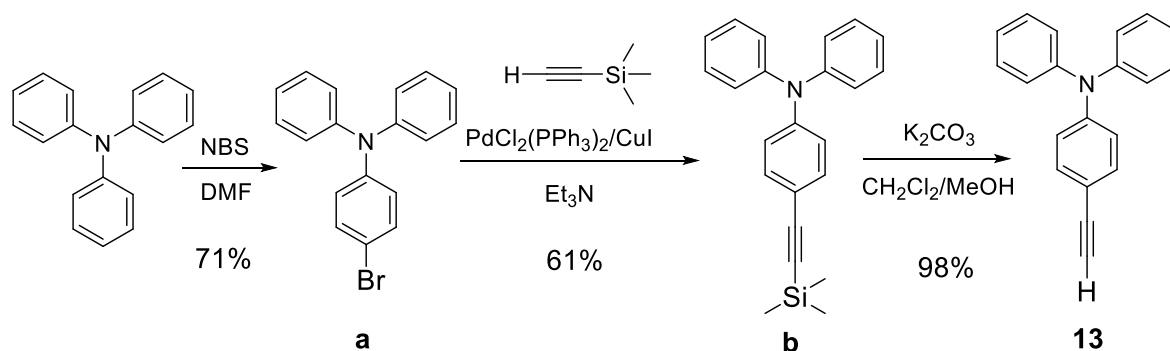

Figure S2. Synthesis of alkyne **13**.
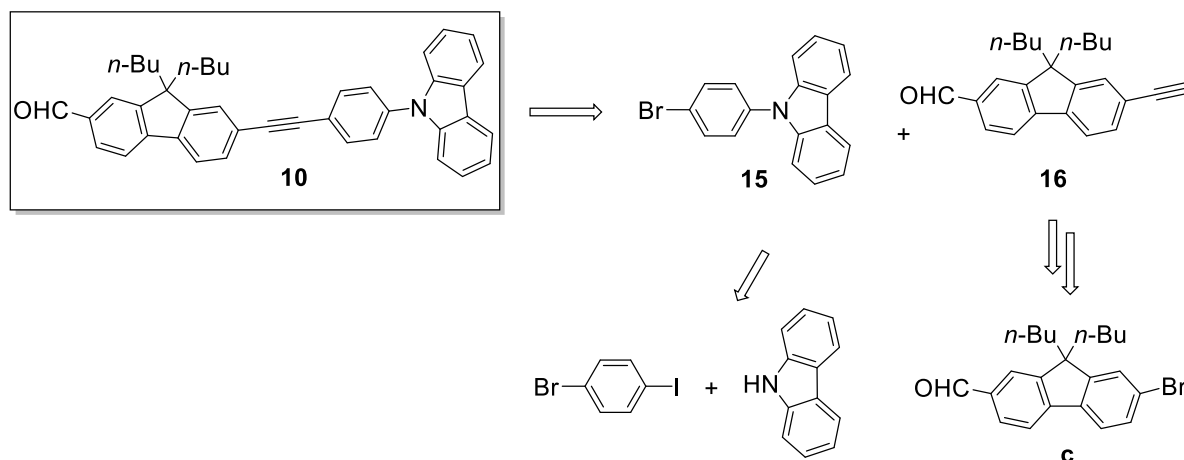
B/ Fluorenylaldehyde 10

Figure S3. Retrosynthetic analysis of fluorenylaldehyde **10** with a carbazole endgroup.

Synthesis of carbazole intermediate c. The first step was the Ullmann Coupling Reaction[31,32] between commercial 1-bromo-4-iodobenzene and 9*H*-carbazole in toluene (Scheme S2), we can note that in order to minimize the formation of doubly substituted arene, it is necessary to use 1-bromo-4-iodobenzene in excess. As described, the bromo derivative **c** was obtained in 86% yield by column chromatography.
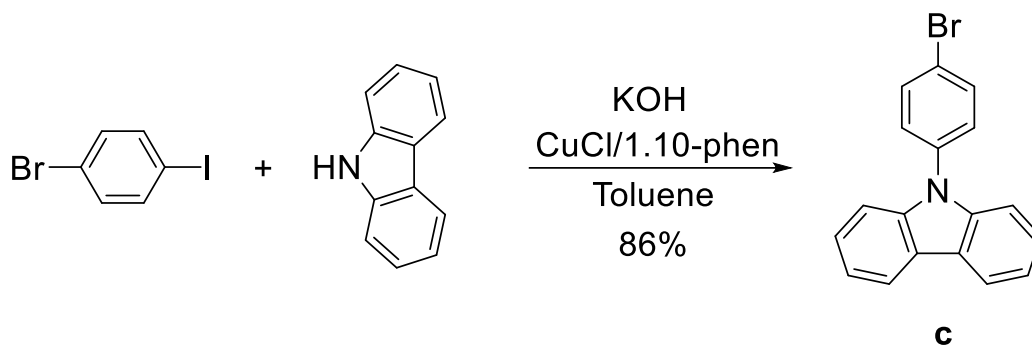

Figure S4. Synthesis of carbazole intermediate **c**.

Synthesis of alkyne 16. On the other hand, alkyne **16** can be obtained by Sonogashira coupling between bromo-derivative **d** and ethynyltrimethylsilane, to give **e** then followed by cleavage of the TMS.[33] In details, intermediate **e** was synthesized in 97% yield from 4-bromofluorene aldehyde **d** by Sonogashira coupling over two days with ethynyltrimethylsilane, and purification by column chromatography on silica gel. Then TMS deprotection of compound **e**

by potassium carbonate, in a mixture of CH_2Cl_2 and MeOH over 12 hours at 45°C, gave **16**, with butyl chains, in 86% yield.
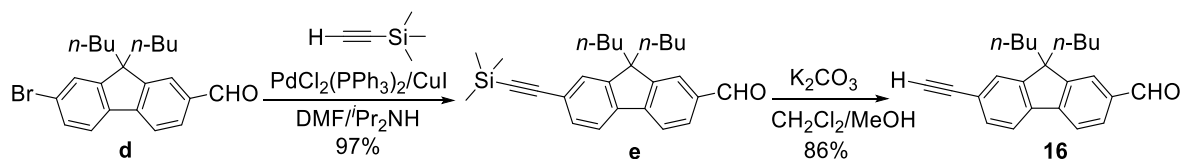

Figure S5. Synthesis of alkyne **16**.
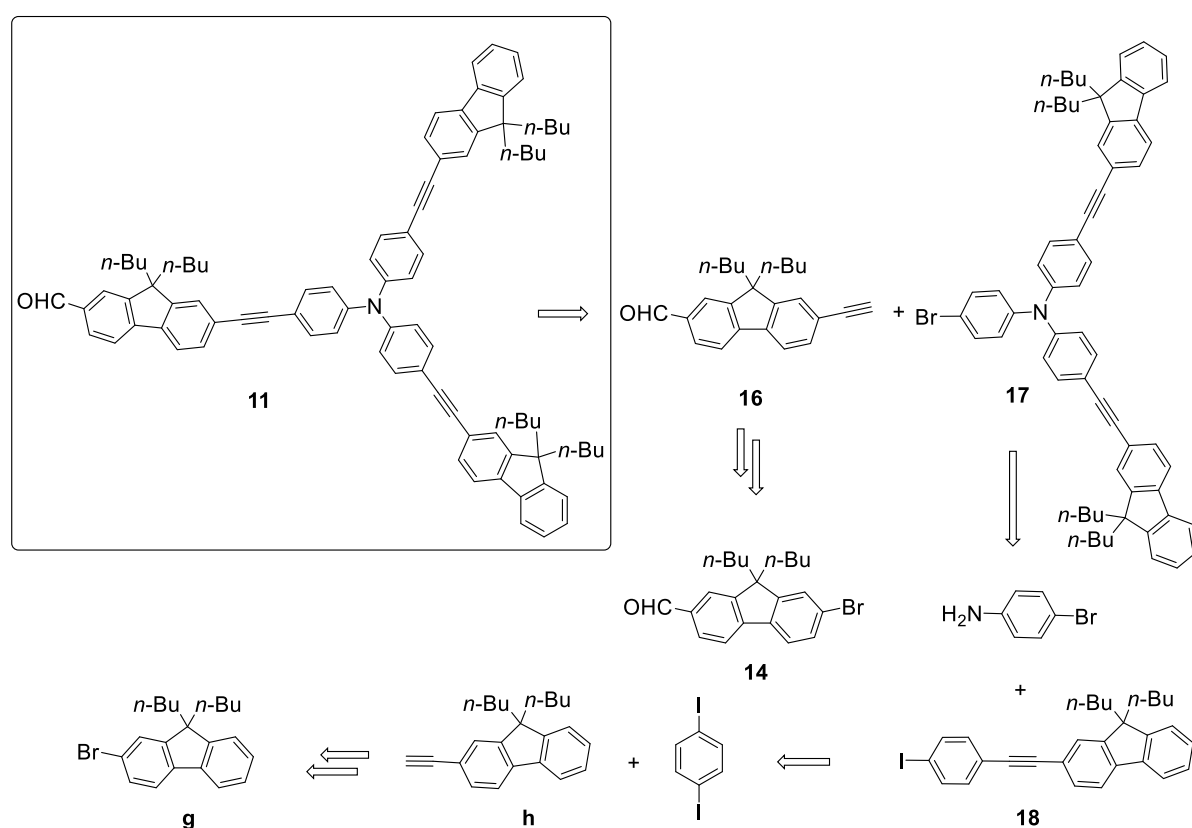
C/ Fluorenylaldehyde 11

Figure S6. Retrosynthetic analysis of aldehyde **11** with junction diphenylamine.

Synthesis of alkyne h. The bromo derivative **g**[12] was reacted with ethynyltrimethylsilane in a Sonogashira coupling to give compound **e**[12] (Figure S7). The derivative **e** was obtained as a red solid in 96% yield after purification by column chromatography (heptane), then deprotection of **e** in a mixture of CH_2Cl_2 and MeOH in the presence of potassium carbonate gave terminal alkyne **h**[12] in 95% yield.
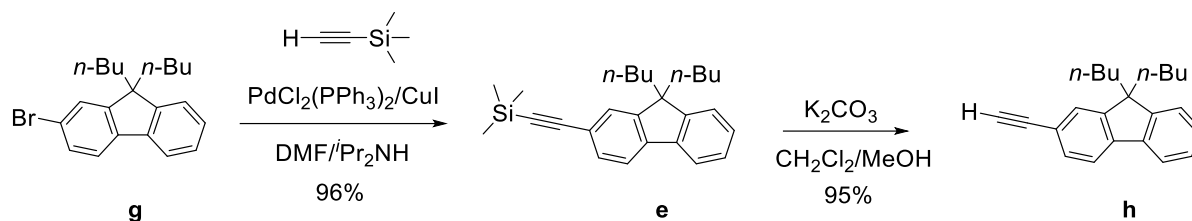
Figure S7. Synthesis of alkyne **h**.

Synthesis of mono-iodo derivative 18. This compound was obtained from commercial 1,4-diiodobenzene and alkyne **h** in a Sonogashira coupling reaction, in 56% yield after purification by column chromatography on silica gel (Figure S8).
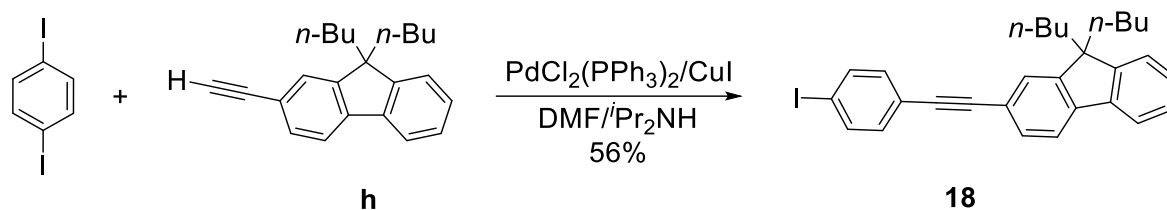
Figure S8. Formation of the iodo derivative **18**.

Synthesis of Bromo derivative 17. This compound was obtained by an Ullmann coupling reaction[31,32] between commercial bromo aniline and iodo compound **18** in 80% yield, after purification by chromatography on silica gel (Figure S9). This reaction proceeds in conditions similar to those used to prepare compound **17**.
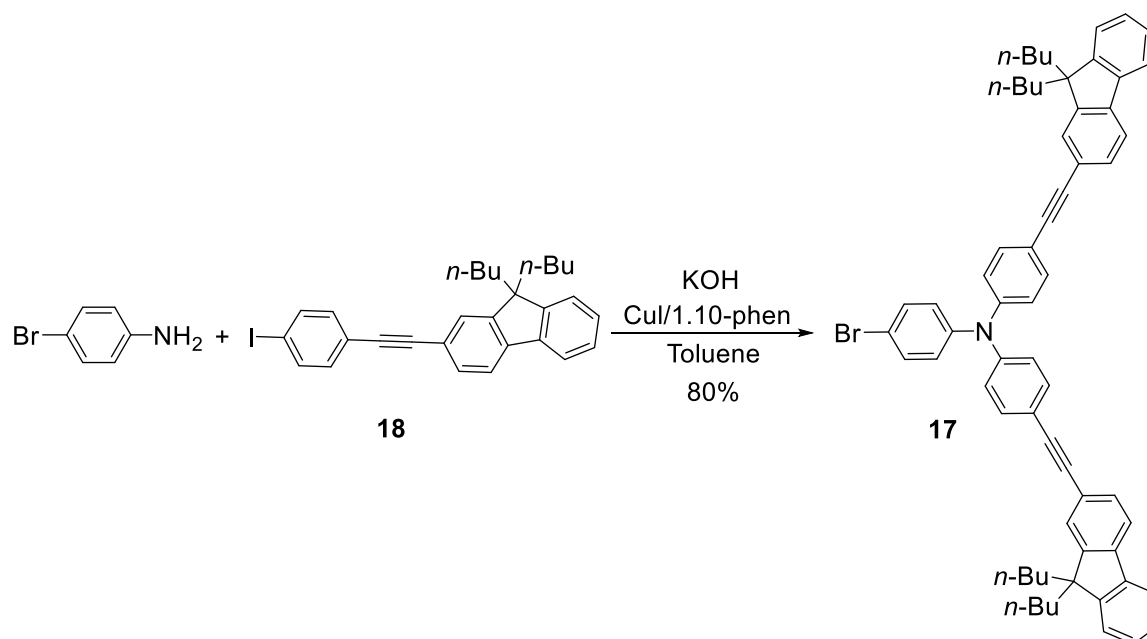

Figure S9. Synthesis of the bromo derivative **17**.
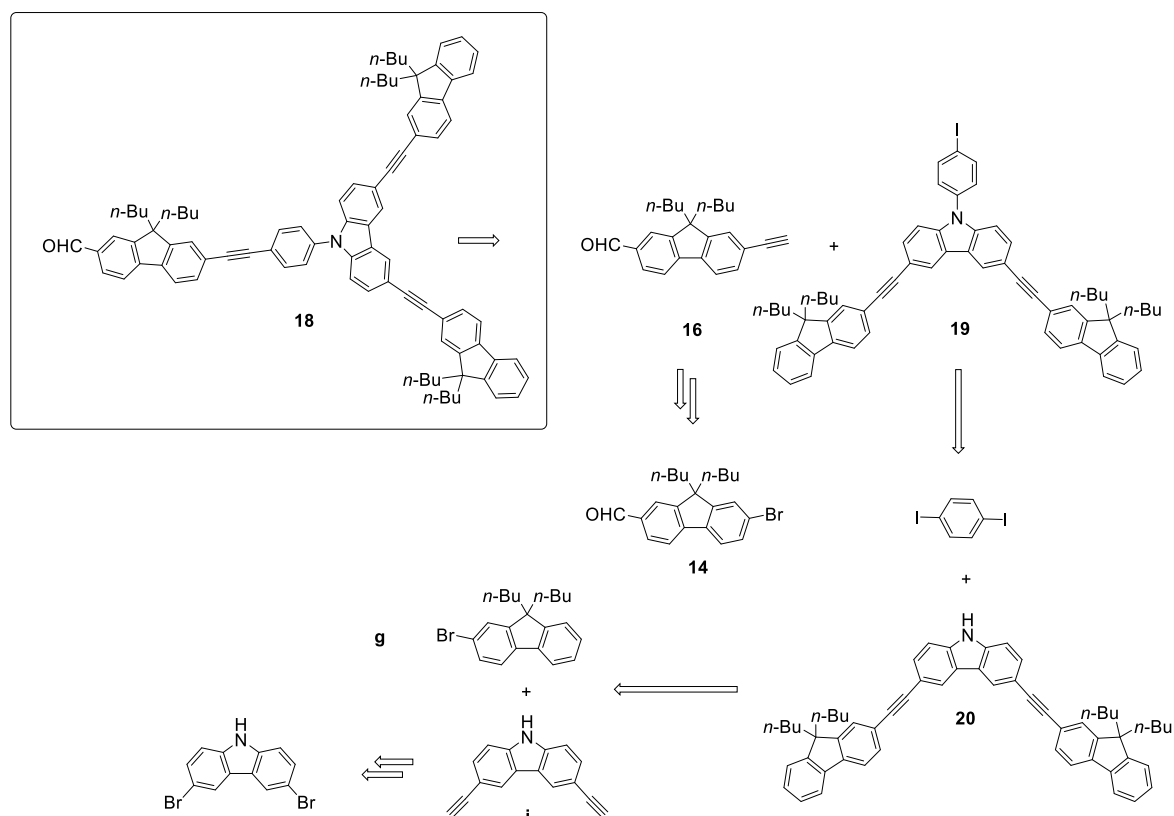
D/ Fluorenylaldehyde 12

Figure S10. Retrosynthetic analysis of aldehyde **19** with a carbazole junction.

Synthesis of bis-alkyne i. This intermediate can be synthesized in two steps from commercially available 3,6-dibromo-9*H*-carbazole, through coupling with ethynyltrimethylsilane followed by removal of the TMS protecting group. In more details; the protected bis-alkyne **j**[20] was synthesized in good yield by Sonogashira coupling between commercial dibromocarbazole and ethynyltrimethylsilane. The deprotection of **j** in basic solution (KOH) gave the free bis-alkyne **i**, as described in the literature.[20] The yield, over the two steps, was 87% after purification by column chromatography (Figure S11).
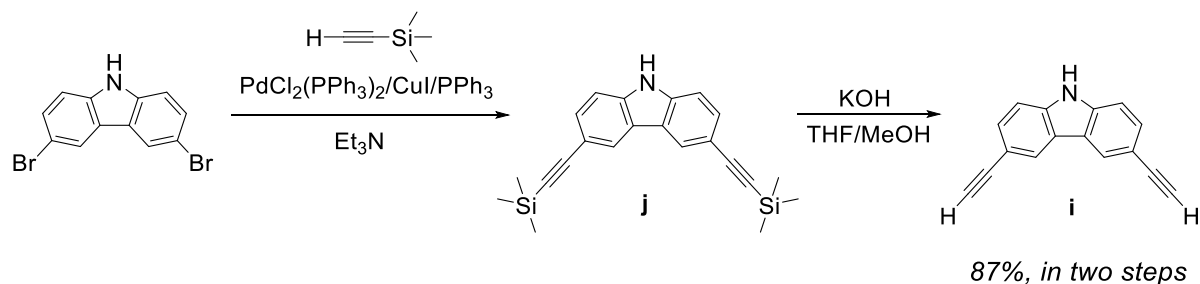

Figure S11. two- step synthesis of bis-alkyne **i**.[20]

Synthesis of compound 20. This compound was obtained under conditions similar to those described earlier for aldehyde **10**: Compound **20** can then be obtained by Sonogashira coupling between alkyne **i** and bromo compound **g**. In this case, in order to improve the yield of this Sonogashira reaction, we used an excess of derivative **g**, which allowed carbazole **20** to be obtained in 58% yield by column chromatography (Figure S12).
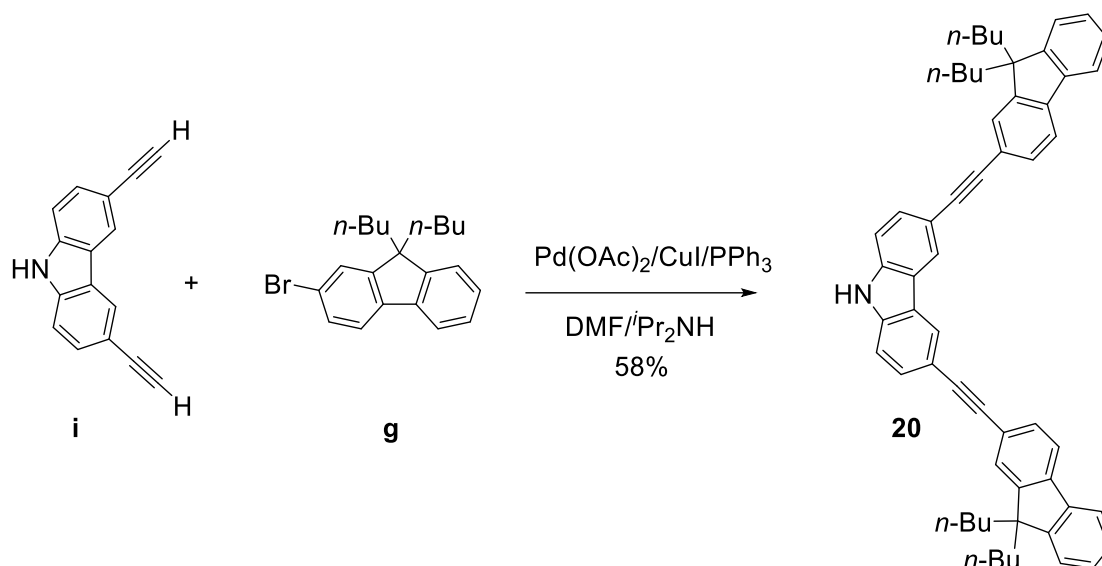
Figure S12. Synthesis of disubstituted carbazole **20**.

Synthesis of 19. An Ullmann coupling of carbazole **20** with 1,4-diiodobenzene can lead to **19** (Figure S13). So, mono-iodo derivative **19** was obtained in 89% yield (after being purified by column chromatography on silica gel), by using conditions similar to those described earlier for compound **17**. We can note that CuI was preferred to CuCl in order to increase the yield.

Figure S13.:Formation of iodo compound **19**.

E/ Synthetic procedures and characterizations for intermediates 17-20

17

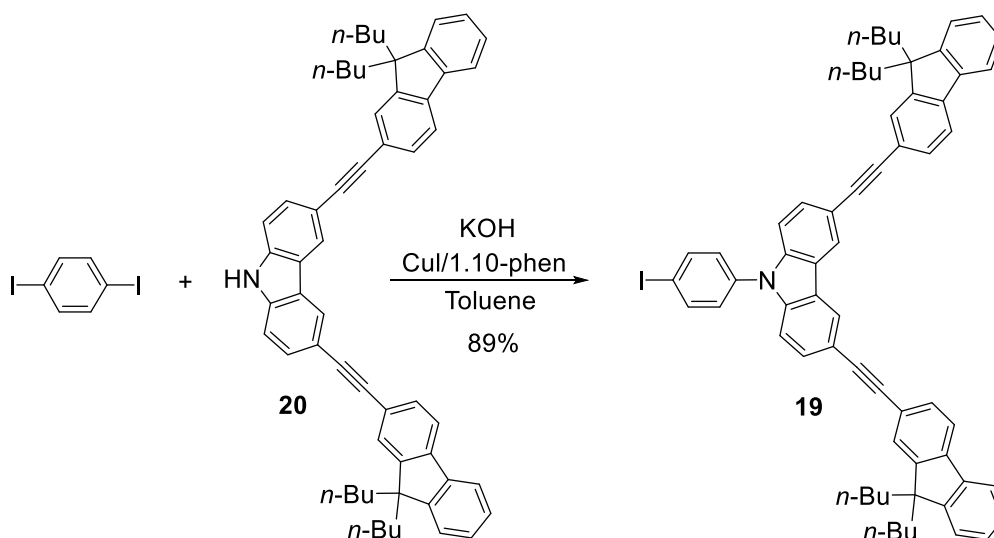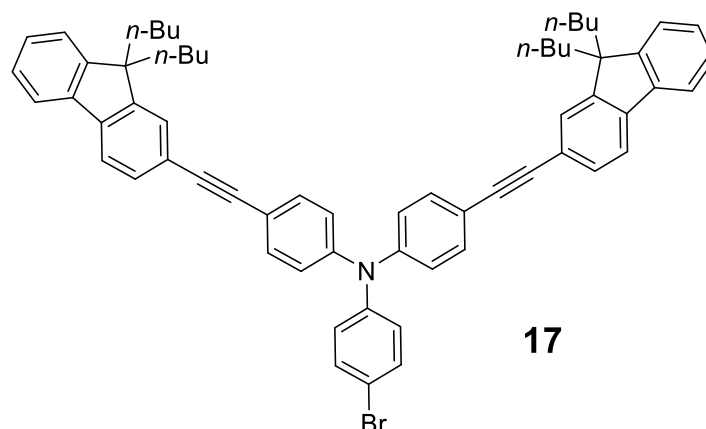**Procedure for 4-Bromo-N,N-bis(4-((9,9-dibutyl-9H-fluoren-2-yl)ethynyl)phenyl)aniline (17).** In a Schlenk tube, a mixture of 9,9-dibutyl-2-((4-iodophenyl)ethynyl)-9*H*-fluorene **26** (1.3 g, 2.56 mmol, 3 eq), 4-bromoaniline (147 mg, 0.85 mmol, 1 eq), 1,10-phenanthroline (15.3 mg, 0.085 mmol, 10% eq), KOH (191 mg, 3.4 mmol, 4 eq) and CuI (16.2 mg, 0.085 mmol, 10% eq) in toluene (20 mL) was stirred at 110 °C for 48 hours under an argon stream. After cooling to room temperature, the mixture was extracted with water and ethyl acetate, the organic layers were separated, and the aqueous layer was extracted with AcOEt (3×100 mL). Then the combined organic phase was washed with water and brine, after the organic layers were dried over anhydrous Na$_2$SO$_4$, filtered and concentrated. Finally, the residue was further purified by chromatography (heptane/CH$_2$Cl$_2$ = 5/1, vol/vol), leading to the title compound as a yellow solid (0.6 g, 80%). ^{1}H NMR (300 MHz, CDCl$_3$, ppm): δ = 7.72-7.66 (m, 4H), 7.52-7.46 (m, 8H), 7.43-7.40 (m, 2H), 7.38-7.31 (m, 6H), 7.08-7.01 (m, 6H), 1.99 (t, *J* = 8.3 Hz, 8H), 1.15-1.03 (m, 8H), 0.69-0.53 (m, 20H).

18
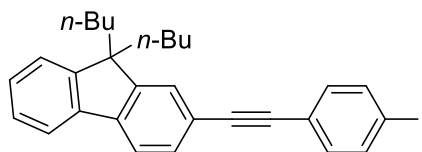
Procedure for 9,9-Dibutyl-2-((4-iodophenyl)ethynyl)-9H-fluorene (18). In a Schlenk tube, a mixture of prepared 9,9-dibutyl-2-ethynyl-9*H*-fluorene **h**[12] (0.8 g, 2.64 mmol, 1 eq), 1,4-diiodobenzene (3.5 g, 10.58 mmol, 4 eq), PdCl$_2$(PPh$_3$)$_2$ (55.5 mg, 0.079 mmol, 3% eq) and CuI (7.6 mg, 0.040 mmol, 1.5% eq) in DMF (7 mL) and ^{i}Pr$_2$NH (7 mL) were stirred at 95 °C for 48 hours under argon atmosphere. After cooling to room temperature, the solvents were evaporated and the residue was further purified by chromatography (heptane), affording the title compound

as a yellow solid (0.7 g, 56%). ^{1}H NMR (300 MHz, CDCl$_3$, ppm): δ = 7.72-7.66 (m, 4H), 7.53-7.50 (m, 2H), 7.36-7.28 (m, 5H), 1.98 (t, J = 8.3 Hz, 4H), 1.12-1.02 (m, 4H), 0.68 (t, J = 7.3 Hz, 6H), 0.63-0.54 (m, 4H).

19
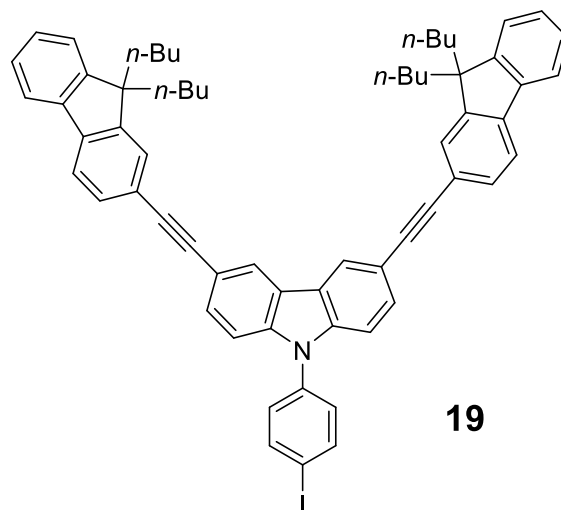
Procedure for 3,6-Bis((9,9-dibutyl-9H-fluoren-2-yl)ethynyl)-9-(4-iodophenyl)-9H-carbazole (19). In a Schlenk tube, a mixture of compound **20** (1.2 g, 1.51 mmol, 1 eq), 1,4-diiodobenzene (1.5 g, 4.52 mmol, 3 eq), 1,10-phenanthroline (27.2 mg, 0.151 mmol, 10% eq), KOH (339 mg, 6.04 mmol, 4 eq) and CuI (28.8 mg, 0.151 mmol, 10% eq) in toluene (18 mL) was stirred at 120 °C for 24 hours under an argon stream. After cooling to room temperature, the mixture was extracted with water and ethyl acetate, then organic layers were separated, and the aqueous layer was extracted with AcOEt (2×100 mL). Then the combined organic layers were washed with water and brine, and the solution was dried over anhydrous MgSO$_4$, filtered and evaporated. Finally, the residue was further purified by chromatography (heptane/CH$_2$Cl$_2$ = 1/1, vol/vol), affording **19** as a yellow solid (1.4 g, 89%). ^{1}H NMR (300 MHz, CDCl$_3$, ppm): δ = 8.44-8.37 (m, 2H), 7.99-7.96 (m, 2H), 7.73-7.57 (m, 10H), 7.38-7.32 (m, 10H), 2.02 (t, J = 16.5, 8.34 Hz, 8H), 1.15-1.05 (m, 8H), 0.72-0.51 (m, 20H).

20
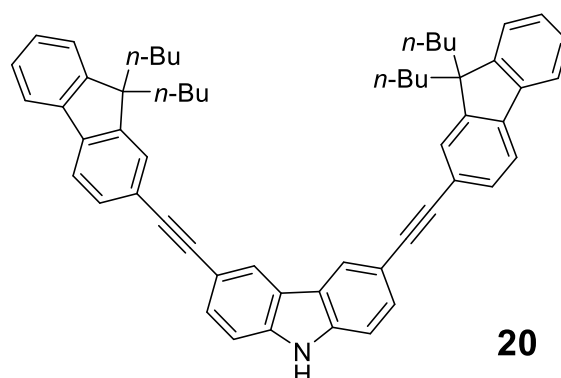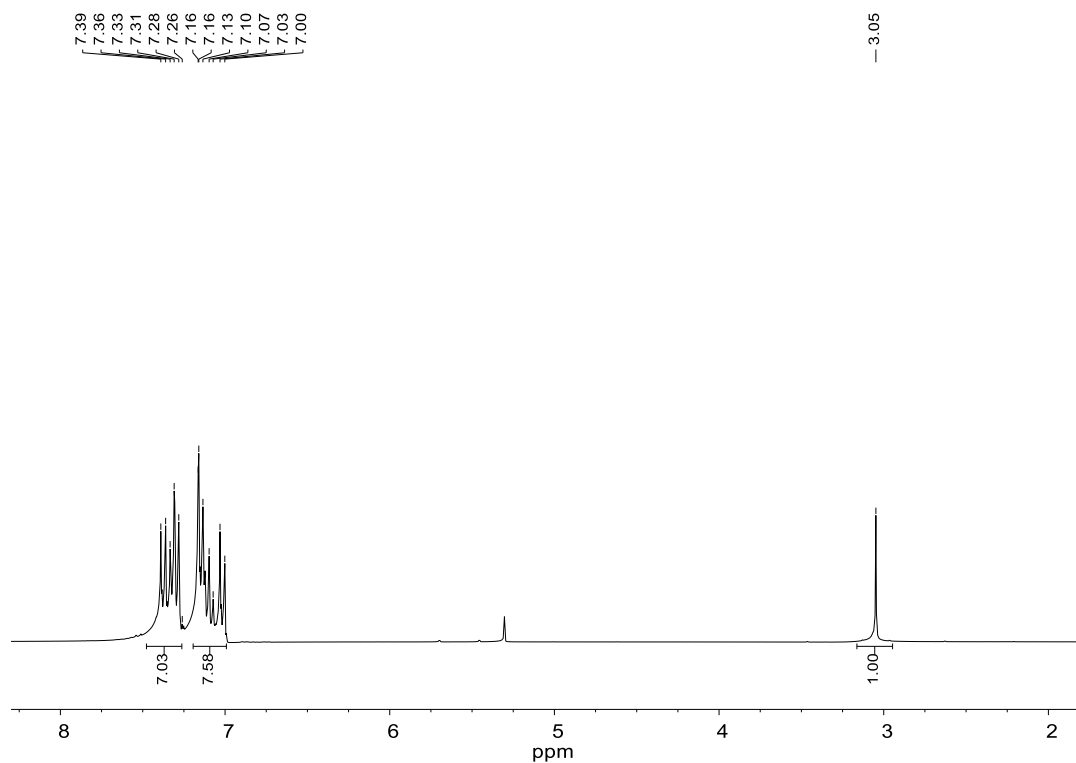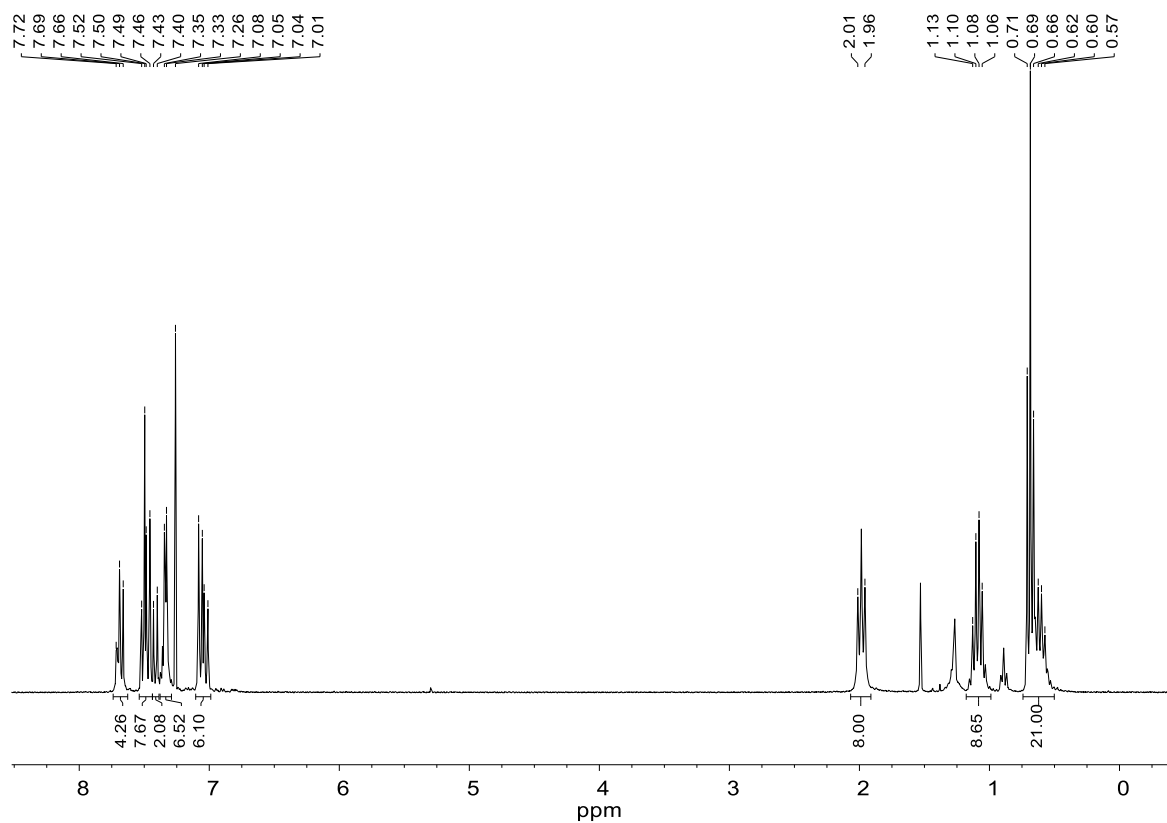
Procedure for 3,6-Bis((9,9-dibutyl-9H-fluoren-2-yl)ethynyl)-9H-carbazole (20). In a Schlenk tube, a mixture of 3,6-diethynyl-9*H*-carbazole **i** (0.56 g, 2.6 mmol, 1 eq), 2-bromo-9,9-dibutyl-9*H*-fluorene **22** (2.8 g, 7.8 mmol, 3 eq), Pd(OAc)$_2$ (14.6 mg, 0.065 mmol, 2.5% eq), CuI (24.8 mg, 0.13 mmol, 5% eq) and PPh$_3$ (34 mg, 0.13 mmol, 5% eq) in DMF (7 mL) and ^{i}Pr$_2$NH (7 mL) were stirred at 100 °C for 48 hours under argon atmosphere. After cooling to room temperature, the solvents were evaporated and the residue was further purified by chromatography (heptane/CH$_2$Cl$_2$ = 1/1, vol/vol), getting yellow solid (1.2 g, 58%). ^{1}H NMR (300 MHz, CDCl$_3$, ppm): δ = 8.33 (s, 2H), 8.24 (s, 1H), 7.73-7.68 (m, 5H), 7.65 (d, *J* = 1.5 Hz, 1H), 7.61-7.56 (m, 4H), 7.42 (d, *J* = 8.4 Hz, 2H), 7.38-7.31 (m, 6H), 2.01 (t, *J* = 16.6, 8.31 Hz, 8H), 1.17-1.05 (m, 8H), 0.72-0.55 (m, 20H).

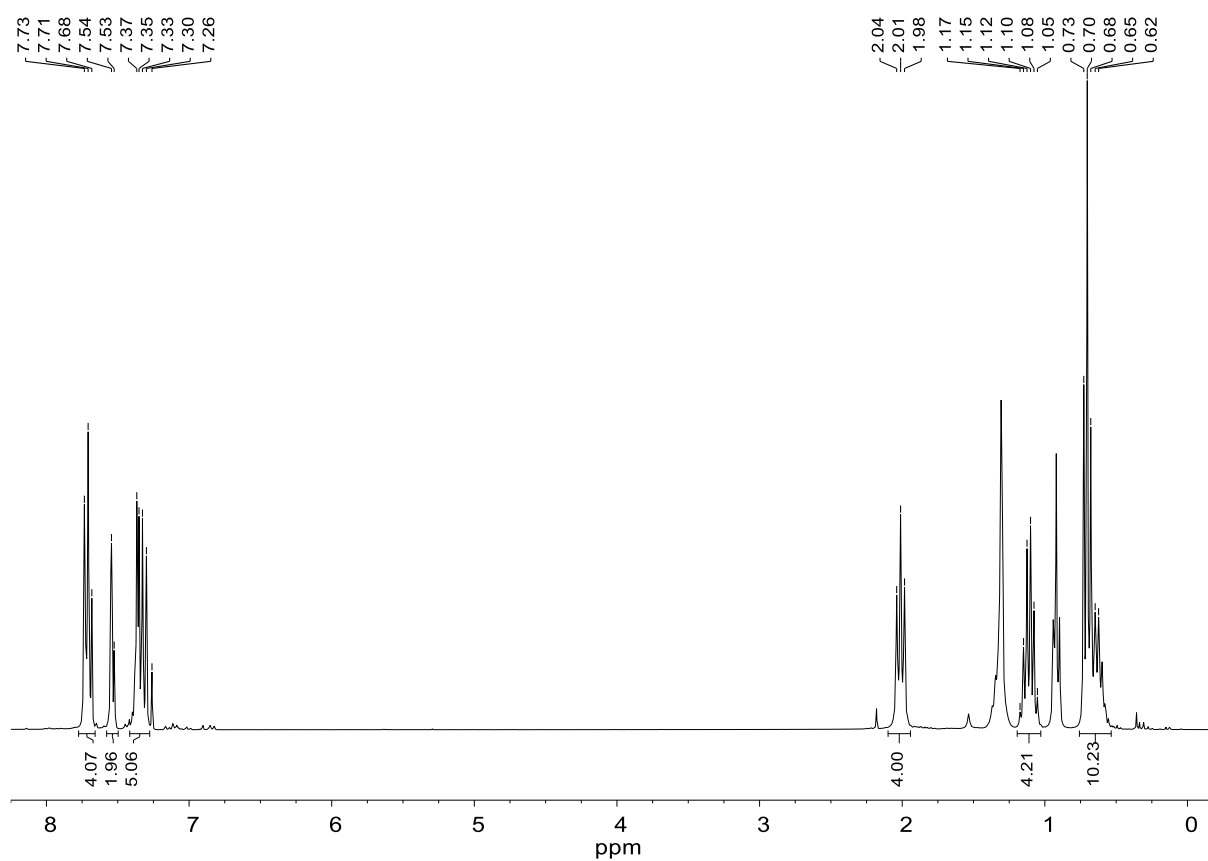## 2. ^{1}H NMR spectra of compounds 13, 17, 18, 19, 20, i and aldehydes 9-12 in CDCl3

Compound 13:

Compound 17:

Compound 18:

Compound 19:
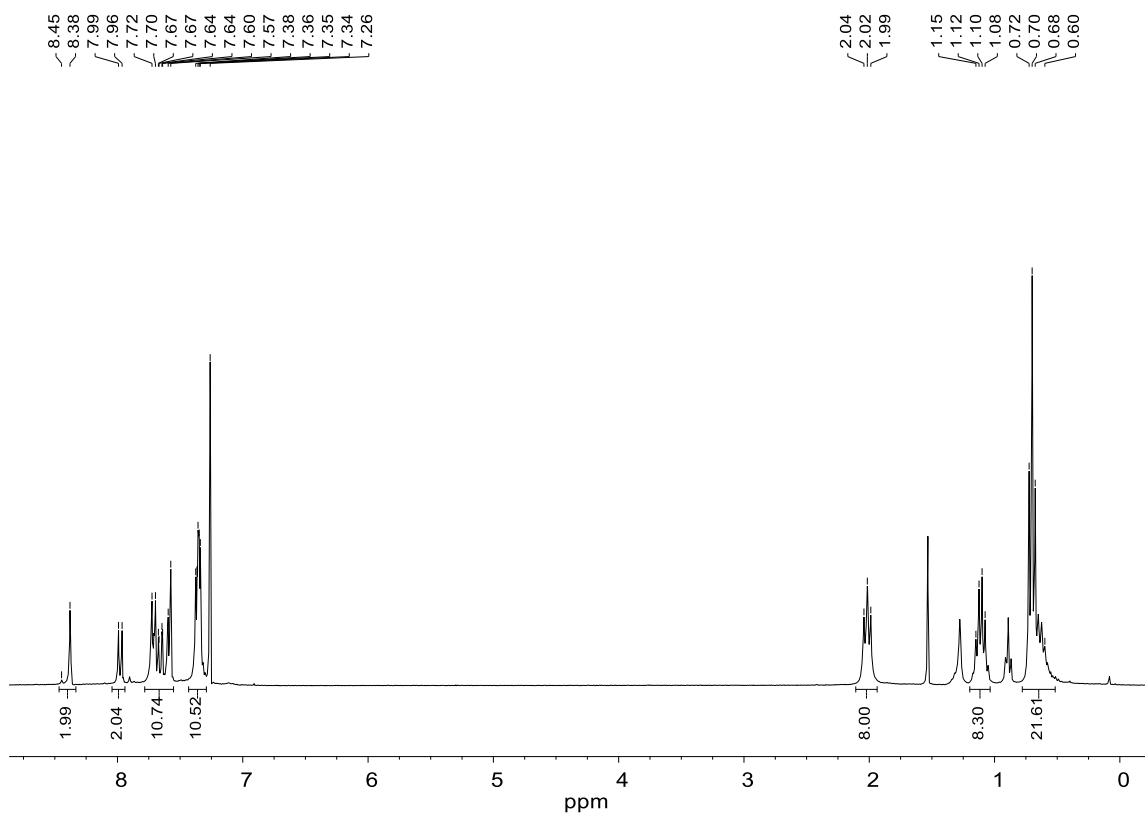
Compound 20:

Compound i:

Aldehyde 9:

10.07

7.88 7.86 7.84 7.82 7.76 7.74 7.55 7.53 7.43 7.41 7.31 7.29 7.27 7.26 7.14 7.12 7.10 7.08 7.04 7.02

2.08 1.99

1.14 1.04 0.69 0.67 0.65 0.50

1.00

3.30 1.05 2.31 2.33 3.51 9.86

4.33

4.36

10.99

Aldehyde 10:

10.09

8.17 8.15 7.91 7.88 7.87 7.83 7.80 7.79 7.64 7.62 7.61 7.46 7.44 7.37 7.34 7.32 7.30 7.26

2.10 2.07 2.05 1.16 1.13 1.11 1.08 0.72 0.70 0.68 0.63 0.58 0.53

1.00

2.14 6.00 4.07 4.34 2.38

4.00

4.01

10.15

Aldehyde 11:

Peak labels (left to right): 10.08

7.89, 7.87, 7.85, 7.78, 7.75, 7.70, 7.67, 7.58, 7.55, 7.52, 7.49, 7.35, 7.33, 7.26, 7.14, 7.11

2.02, 1.99, 1.97, 1.14, 1.11, 1.09, 1.06, 0.71, 0.69, 0.66, 0.63, 0.61, 0.58

Integrals: 1.00 | 3.36, 1.26, 4.23, 12.18, 6.34, 6.00 | 12.58 | 12.89 | 32.38

Aldehyde 12:

Peak labels (left to right): 10.09

8.40, 7.91, 7.88, 7.86, 7.84, 7.80, 7.73, 7.70, 7.67, 7.66, 7.64, 7.62, 7.61, 7.58, 7.45, 7.42, 7.36, 7.34, 7.26

2.11, 2.05, 2.02, 1.99, 1.15, 1.13, 1.10, 1.08, 0.73, 0.70, 0.68, 0.63, 0.60

Integrals: 1.00 | 2.01 | 6.76, 5.65, 10.03, 2.44, 7.09 | 13.10 | 14.24 | 33.94

3. ^{13}C NMR spectra of aldehydes 9-12

Aldehyde 9:

Aldehyde 10:

Aldehyde 11:

192.23
152.22
151.80
151.01
150.77
146.91
146.77
146.56
141.37
140.44
139.56
135.57
132.84
132.79
130.83
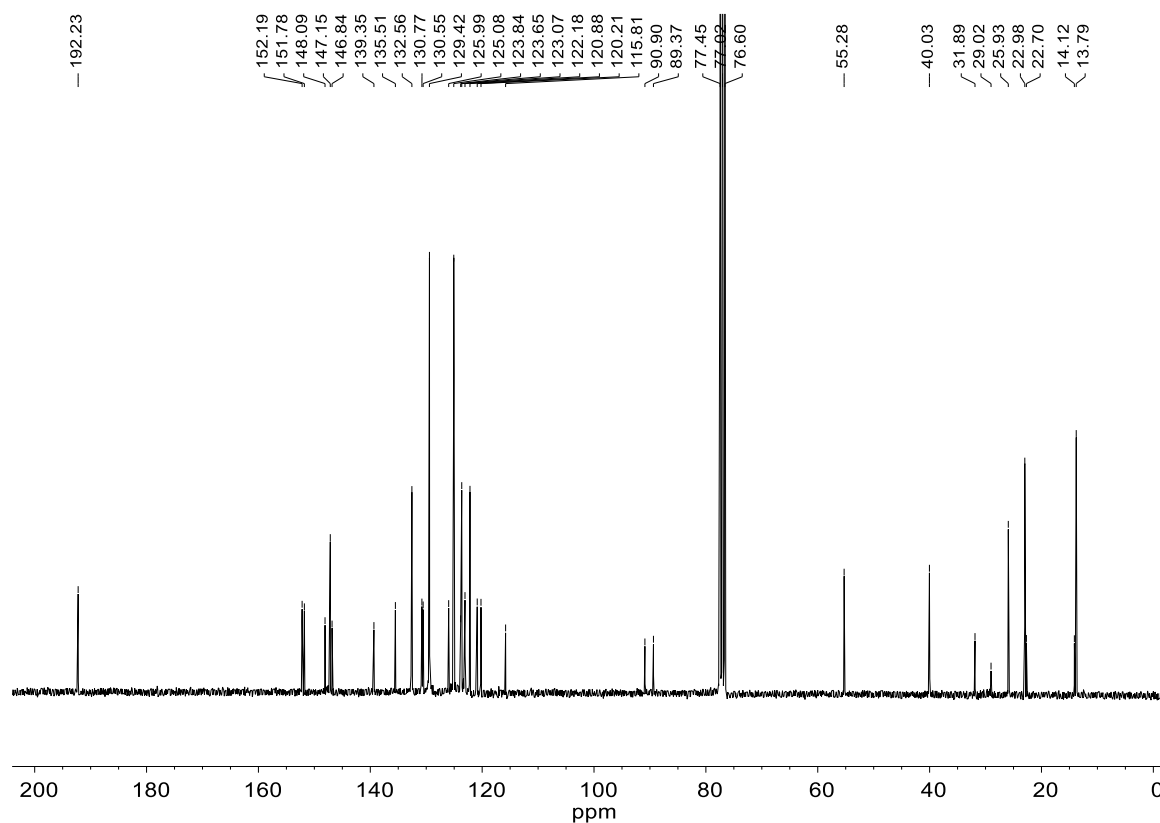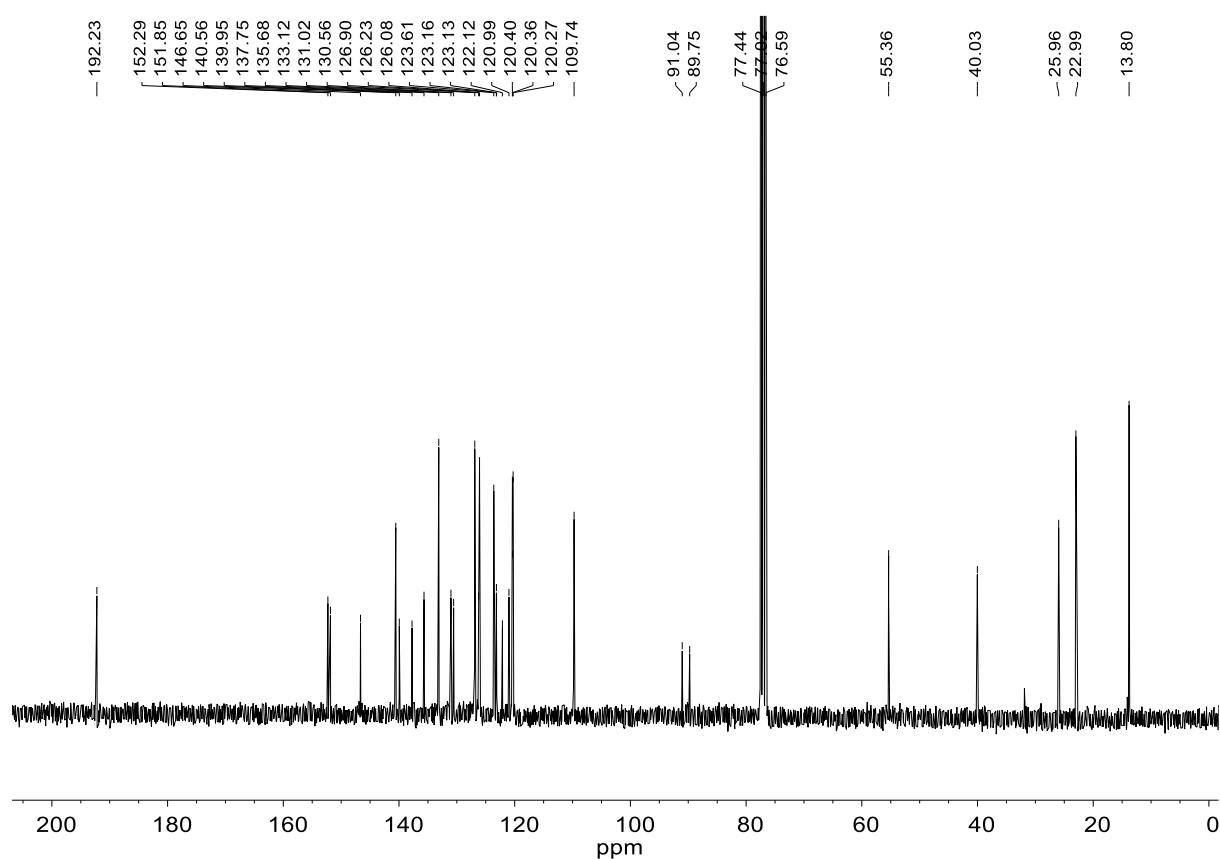130.53
127.49
126.88
126.06
125.88
124.17
123.92
123.59
123.09
122.90
121.50
120.92
120.26
119.97
119.63
118.30
117.67
90.57
90.46
90.04
89.20
55.31
55.06
40.20
40.03
31.89
29.02
25.93
23.07
22.98
22.70
14.11
13.79

Aldehyde 12:

192.27
152.32
151.86
151.03
150.80
146.63
141.24
140.53
140.07
136.84
135.71
133.29
131.09
130.60
130.54
130.14
127.46
126.89
126.26
125.90
124.13
123.30
123.14
123.03
122.91
122.88
121.78
121.04
120.41
119.97
119.68
115.64
110.11
91.47
90.24
89.53
89.48
55.39
55.10
40.28
40.05
25.96
23.12
23.01
22.72
13.86
13.83

4. ¹H NMR spectra of porphyrins 1-8 in CDCl₃

Porphyrin 1:

Porphyrin 2:

Porphyrin 3:
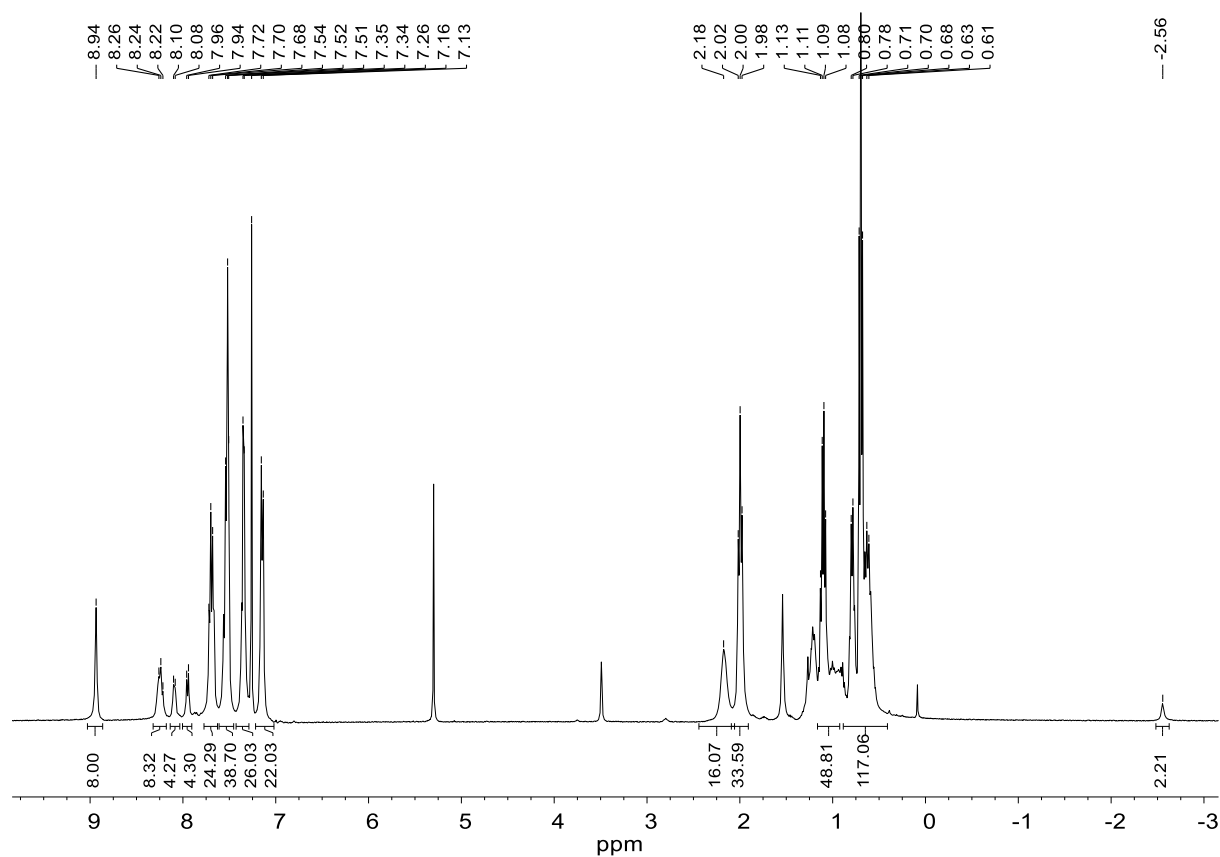
Porphyrin 4:
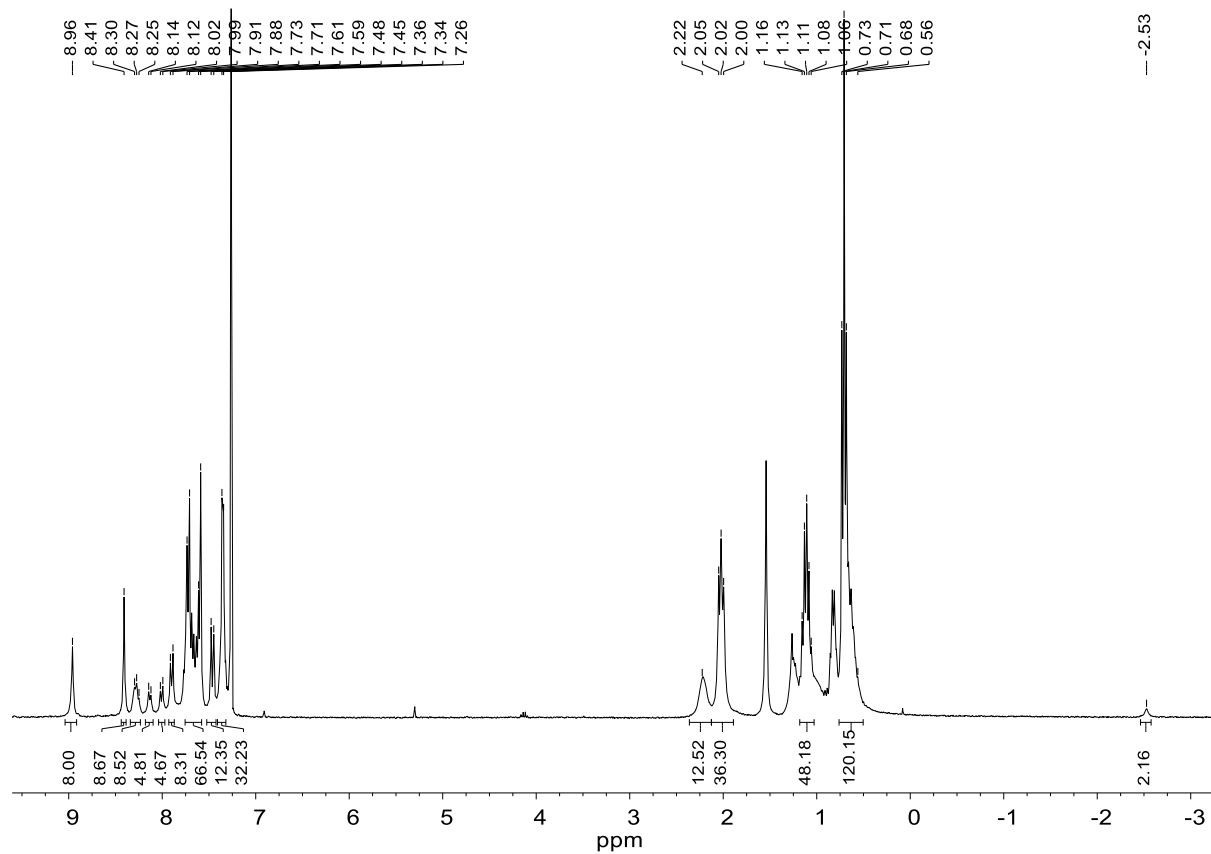
Porphyrin 5:

Porphyrin 6:

Porphyrin 7:

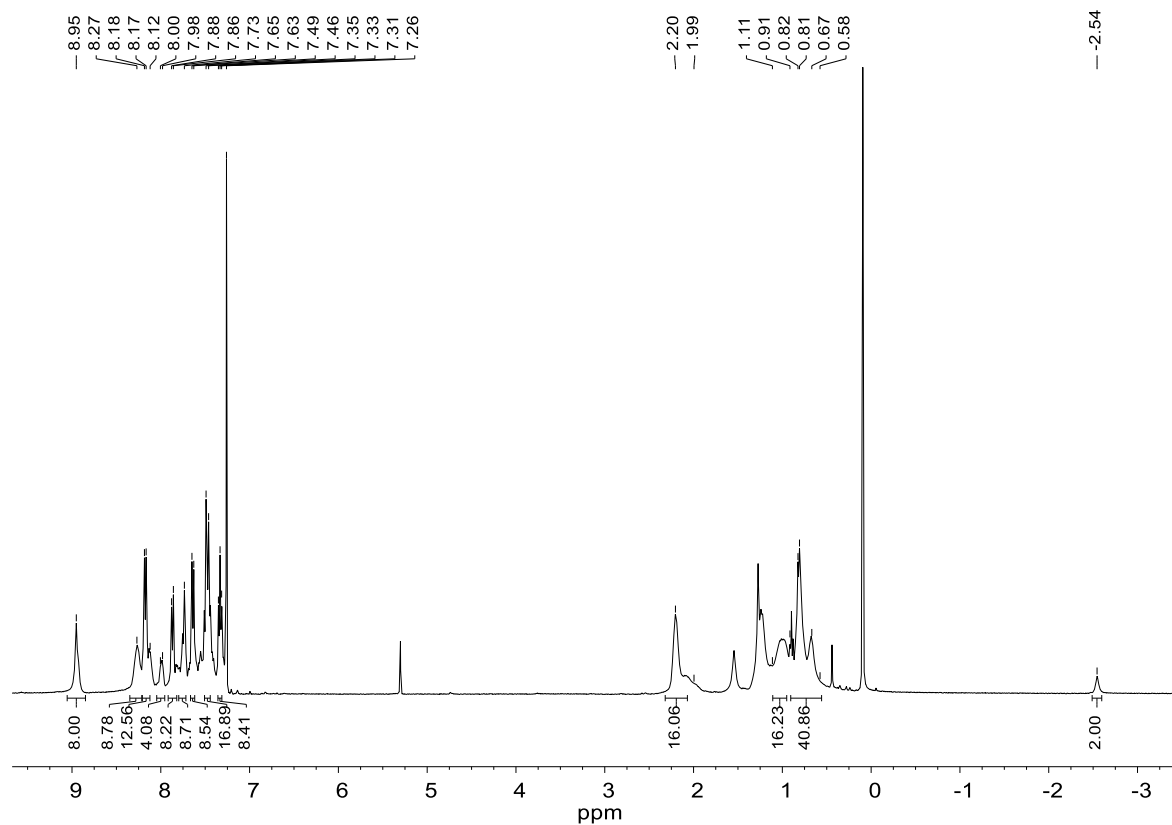9.04 | 8.26 8.10 8.08 7.96 7.94 7.70 7.67 7.53 7.52 7.35 7.26 7.16 7.13 | 2.17 2.02 2.00 1.97 1.14 1.12 1.09 1.07 0.81 0.78 0.72 0.70 0.67 0.61 0.59

8.00 | 8.47 4.30 4.97 24.54 41.45 26.70 22.80 | 16.78 32.85 | 48.39 | 119.45

ppm

Porphyrin 8:

9.07 | 8.41 8.29 8.15 8.01 7.90 7.72 7.60 7.47 7.44 7.35 7.26 | 2.22 2.02 | 1.11 0.83 0.71

8.00 | 8.53 4.90 4.36 5.27 8.94 58.49 11.63 30.46 | 16.32 35.74 | 49.76 | 120.60

ppm
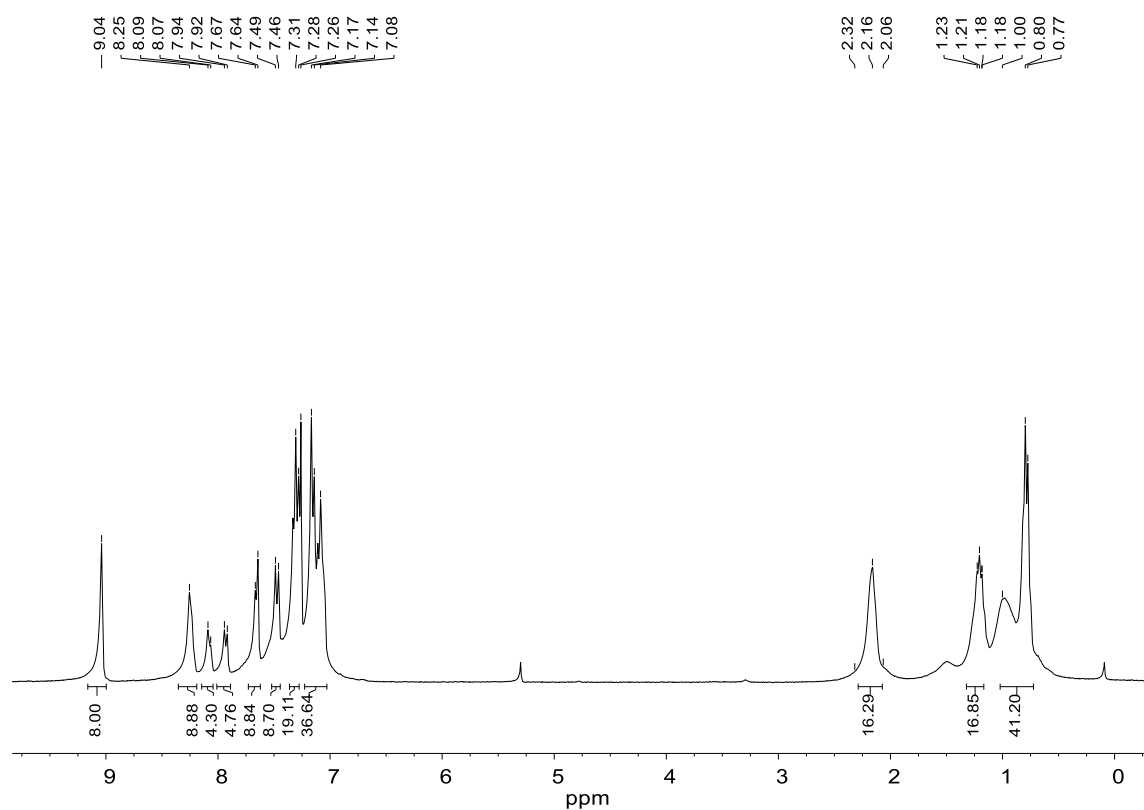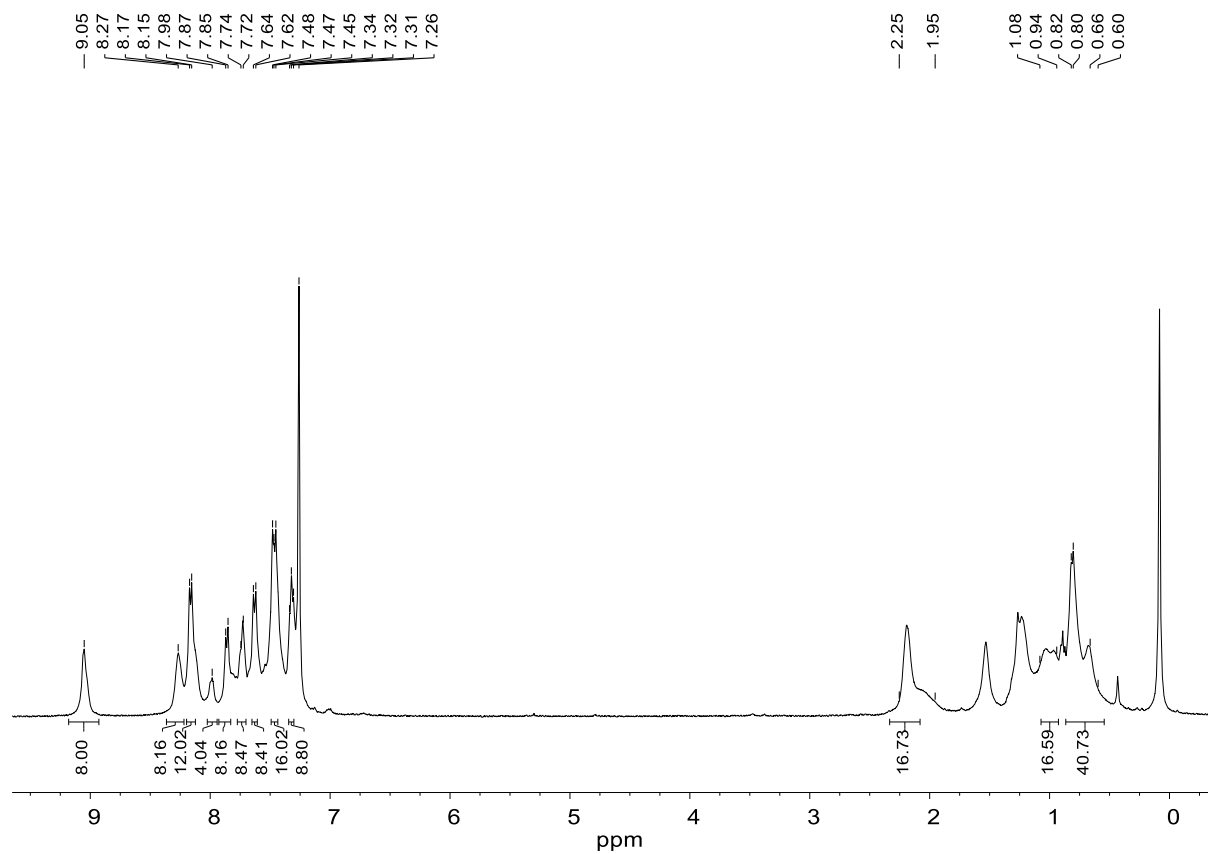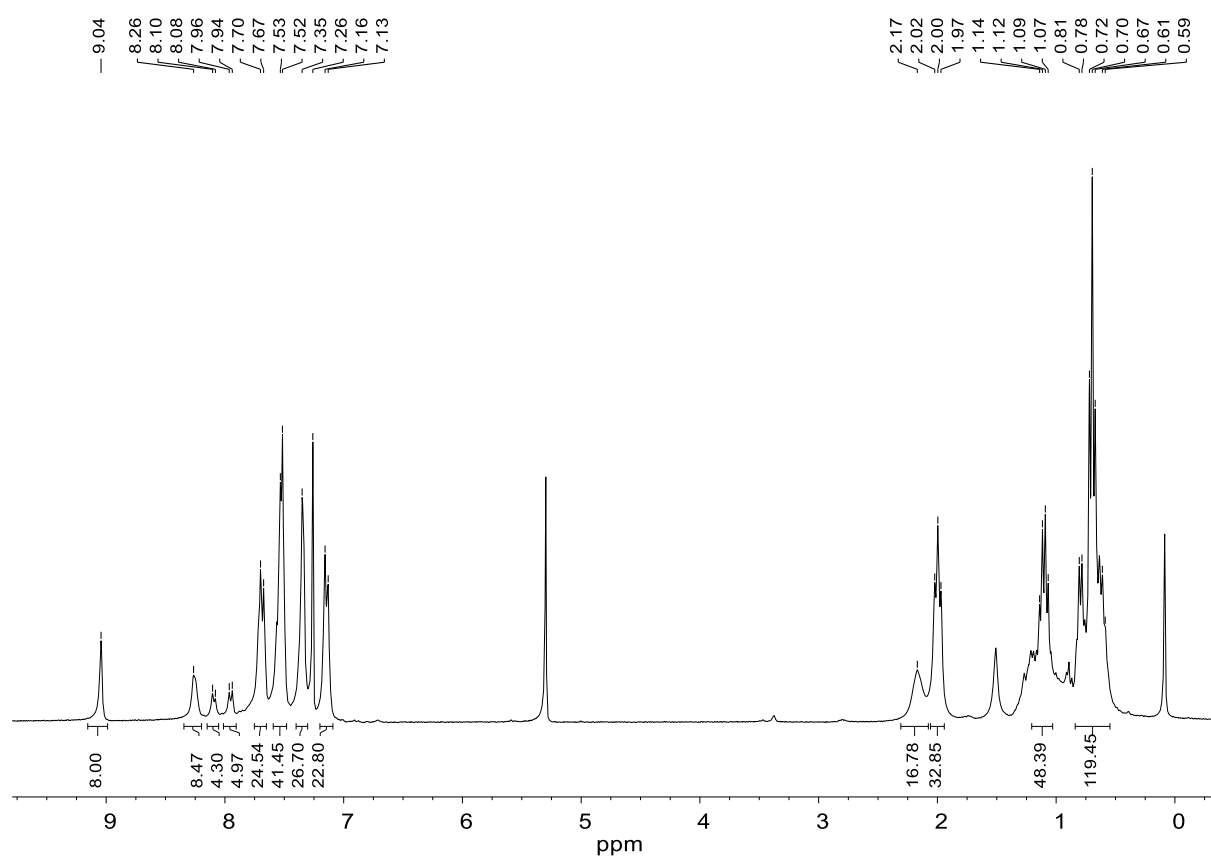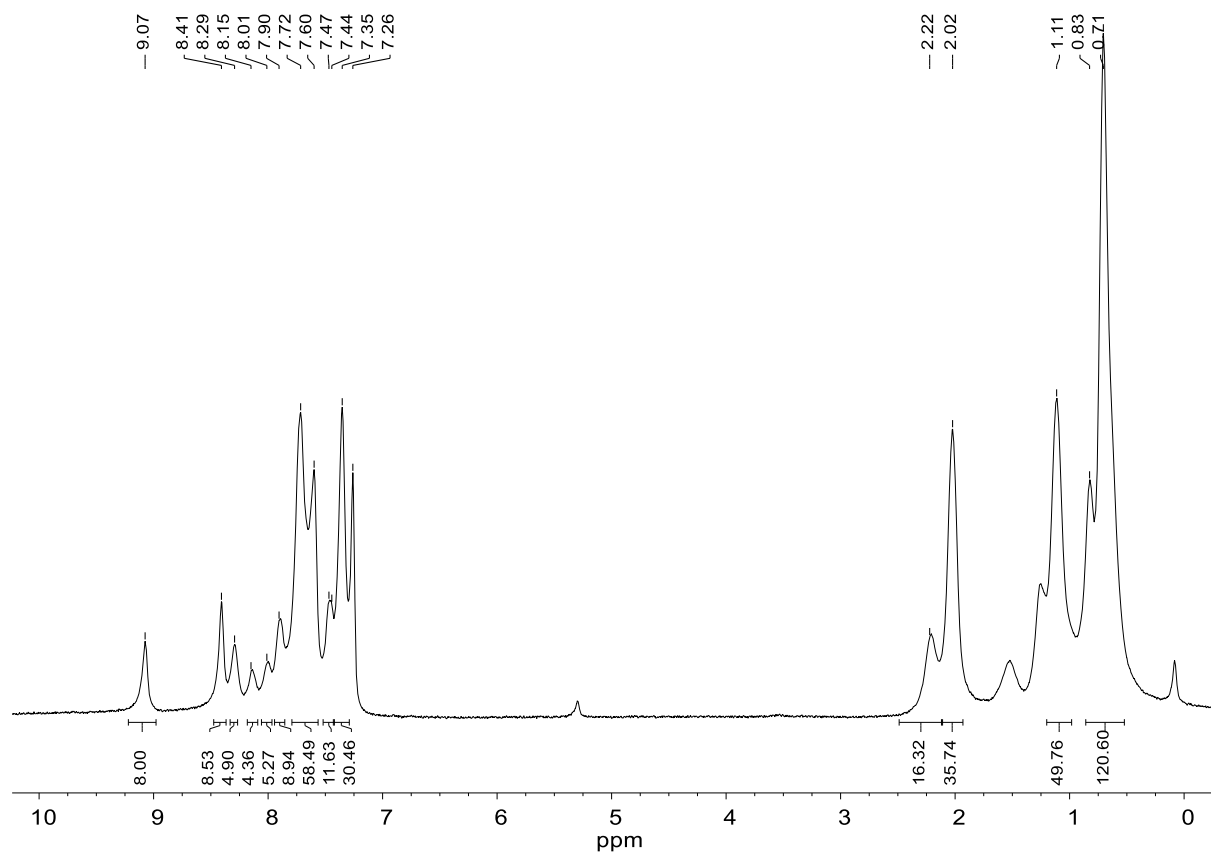
5. Comparison of ^{1}H NMR spectra of porphyrins 1-8

Diphenylamine series. The complete spectra of porphyrins **1,3,4,6** was overlayed. For clarity, we now divide the full spectra into two parts: (Figure S14a: between 6.6 ppm and 9.2 ppm) and (Figure S14b: between -3.0 ppm and 2.5 ppm). The integration shows eight protons around 9 ppm, which are assigned to β-pyrrole protons (H_β) of the porphyrin macrocycle. We notice that the H_β protons are found to lower field in the zinc porphyrins (going from 8.9 ppm to 9.1 ppm). For the aromatic protons, we can clearly distinguish three proton signals ($H_{A,B,C}$) between 7.9 and 8.3 ppm that belong to the four distinct aromatic protons of the *meso*-fluorenyl spacers, and which integrate in total for sixteen protons. Figure S14b shows the partial spectra between -3.0 and 2.5 ppm. The singlet at -2.6 ppm is from the –N*H* functionalities that lie inside porphyrin macrocycle; these are absent for zinc porphyrins, where they are replaced by the Zn(II) ion. The *n*-butyl chains could also be identified between 0.5 and 2.2 ppm.
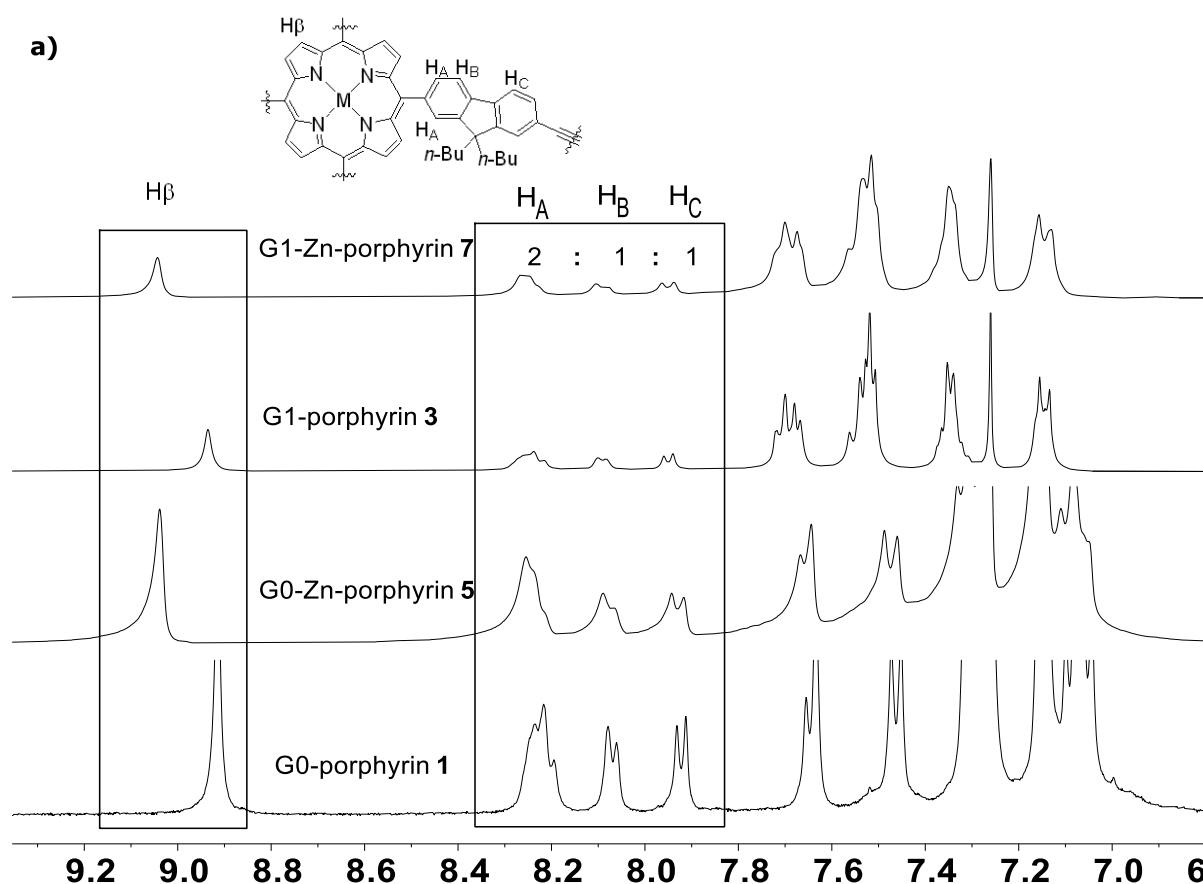
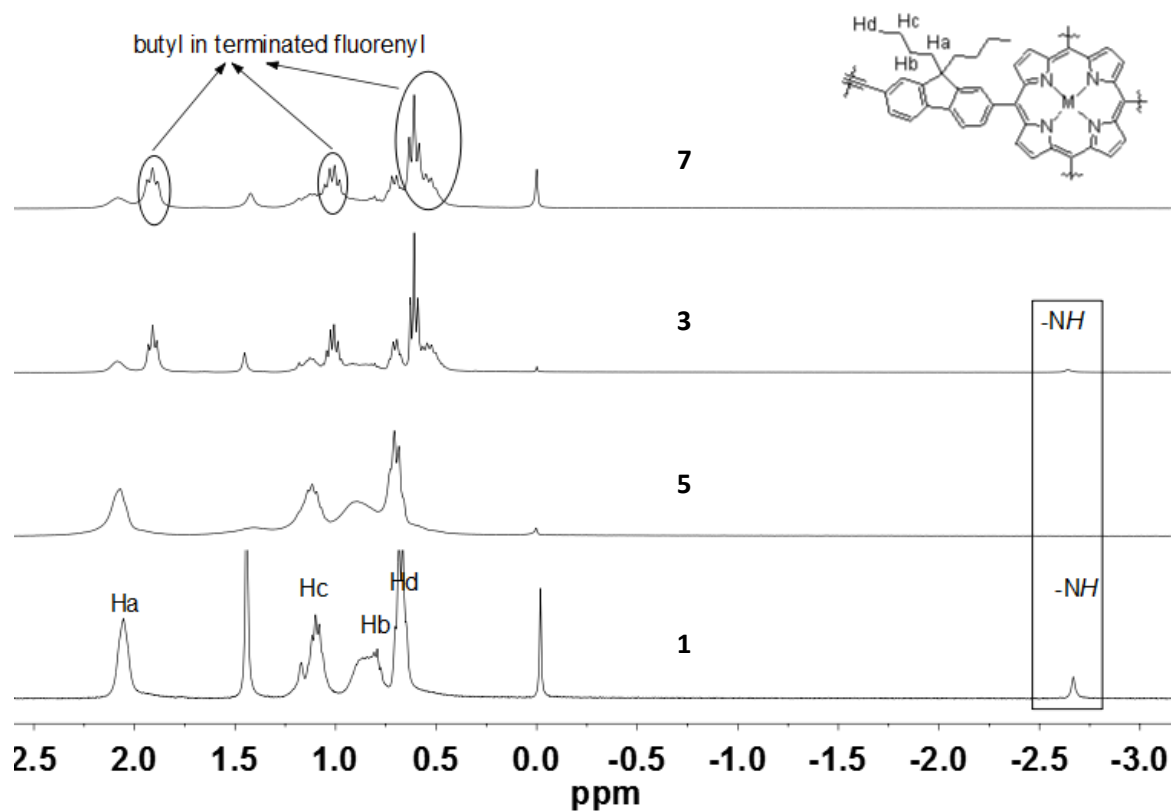**b)**

Figure S14. a) Partial ^{1}H NMR spectra of porphyrins **1**, **3**, **5** and **7** at low field (7-9.2 ppm); **b)** Partial ^{1}H NMR spectra of porphyrins **1**, **3**, **5** and **7** at high field (-3.0- 2.5 ppm).

6. Partial ^{1}H NMR spectra of porphyrin 4

The detailed ^1H NMR spectrum of free-base porphyrin **3**, given in Figure S15 (between 7.0-9.3 ppm). For the aromatic protons: (i) there are eight protons at 8.4 ppm, which are assigned to H_D carbazole protons, and (ii) there are three proton signals $H_{A,B,C}$ between 7.9 and 8.4 ppm, belonging to the aromatic protons of the *meso*-fluorenyl spacers. The same results are observed for the corresponding zinc complex **8** but, as before, we notice that the peaks are broader.
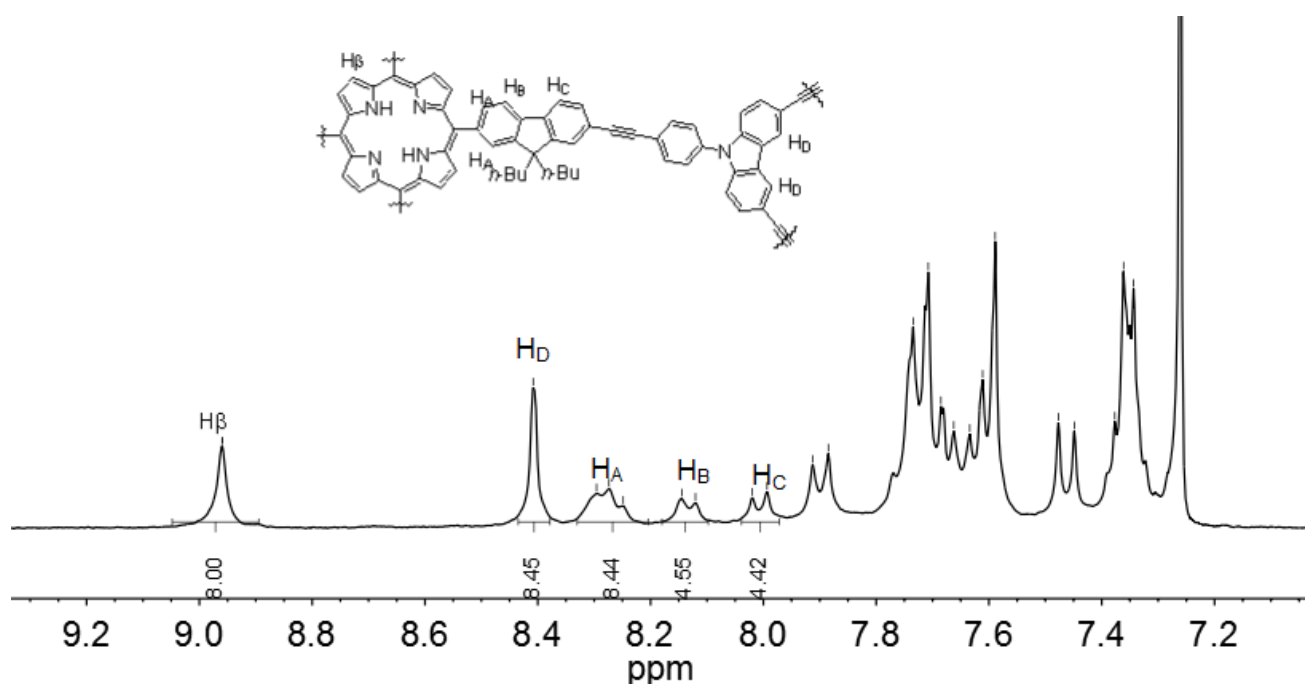

Figure S15. Partial ^{1}H NMR spectra of porphyrin **4** (7.2-9.2 ppm).

7. $^{13}C\{^1H\}$ NMR spectra for porphyrins 1-8 in CDCl$_3$

Porphyrin 1:

Peak labels: 151.30, 149.56, 147.94, 147.26, 141.35, 140.97, 140.18, 133.81, 132.58, 130.86, 129.43, 126.06, 125.04, 123.58, 122.39, 122.31, 120.75, 120.07, 118.18, 116.28, 90.07, 89.85, 77.45, 77.03, 76.61, 55.40, 40.34, 26.38, 23.16, 14.04, 13.99

Porphyrin 2:

Peak labels: 151.41, 149.60, 141.54, 140.60, 140.07, 140.05, 137.57, 133.84, 133.12, 132.77, 132.04, 131.11, 129.44, 126.93, 126.25, 126.10, 126.01, 123.60, 122.44, 121.65, 120.69, 120.41, 120.26, 120.09, 118.32, 109.80, 91.55, 89.06, 77.35, 77.03, 76.72, 55.47, 40.33, 34.15, 29.74, 26.40, 23.17, 22.37, 14.09, 14.07, 14.02

Porphyrin 3:

Peak labels (left to right): 151.03, 150.77, 146.73, 146.65, 141.35, 141.16, 140.46, 132.80, 130.54, 127.49, 126.89, 125.90, 124.12, 124.07, 122.91, 122.04, 121.53, 120.72, 119.98, 119.64, 118.19, 118.08, 90.53, 89.25, 77.34, 77.02, 76.71, 55.41, 55.07, 40.22, 26.36, 25.93, 23.14, 23.09, 14.03, 13.99, 13.84

Porphyrin 4:

Peak labels (left to right): 151.47, 151.06, 150.83, 149.68, 141.66, 141.61, 141.25, 140.60, 140.56, 140.08, 136.69, 133.29, 130.58, 130.18, 127.47, 126.91, 125.93, 124.11, 123.32, 123.21, 122.92, 121.84, 121.60, 120.75, 119.99, 119.70, 115.65, 110.16, 92.01, 90.31, 89.51, 88.90, 77.47, 77.05, 76.62, 55.51, 55.12, 53.43, 40.29, 26.40, 25.98, 23.13, 14.08, 14.04, 13.88

Porphyrin 5:

151.26, 150.40, 149.40, 147.91, 147.25, 141.93, 141.06, 139.99, 133.56, 132.55, 131.98, 130.82, 129.41, 126.01, 125.01, 123.55, 122.37, 122.19, 121.76, 119.99, 118.03, 116.28; 89.98, 89.84; 77.43, 77.01, 76.59; 55.37; 40.35; 26.35, 23.16, 23.14; 14.02, 13.97

Porphyrin 6:

151.37, 150.37, 149.44, 142.16, 141.63, 140.58, 137.53, 133.59, 133.10, 131.97, 131.08, 126.92, 126.23, 126.07, 123.58, 122.45, 121.55, 120.39, 120.23, 120.12, 120.07, 118.19, 109.86, 109.76, 91.56, 89.00; 77.34, 77.22, 76.70; 55.43; 40.38, 40.21; 29.72, 26.43, 23.19, 22.35; 14.07, 14.02

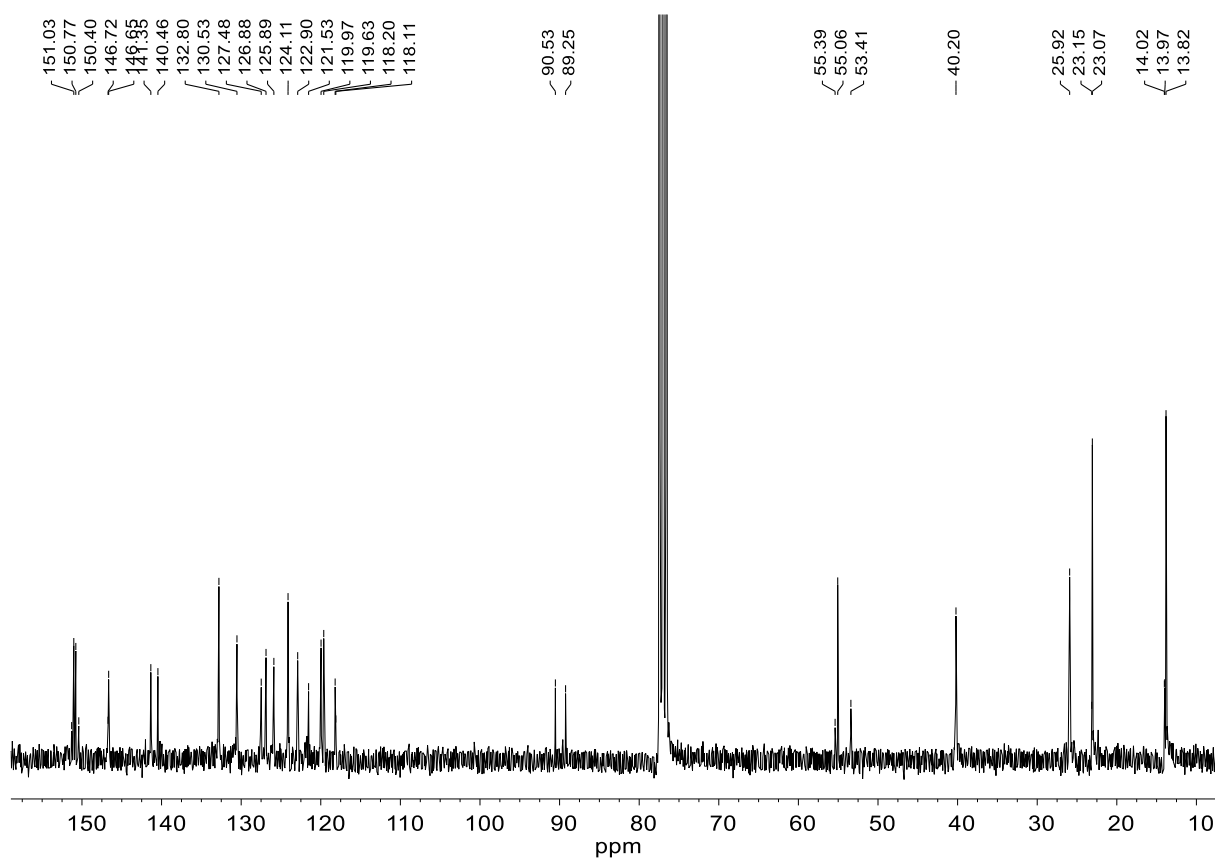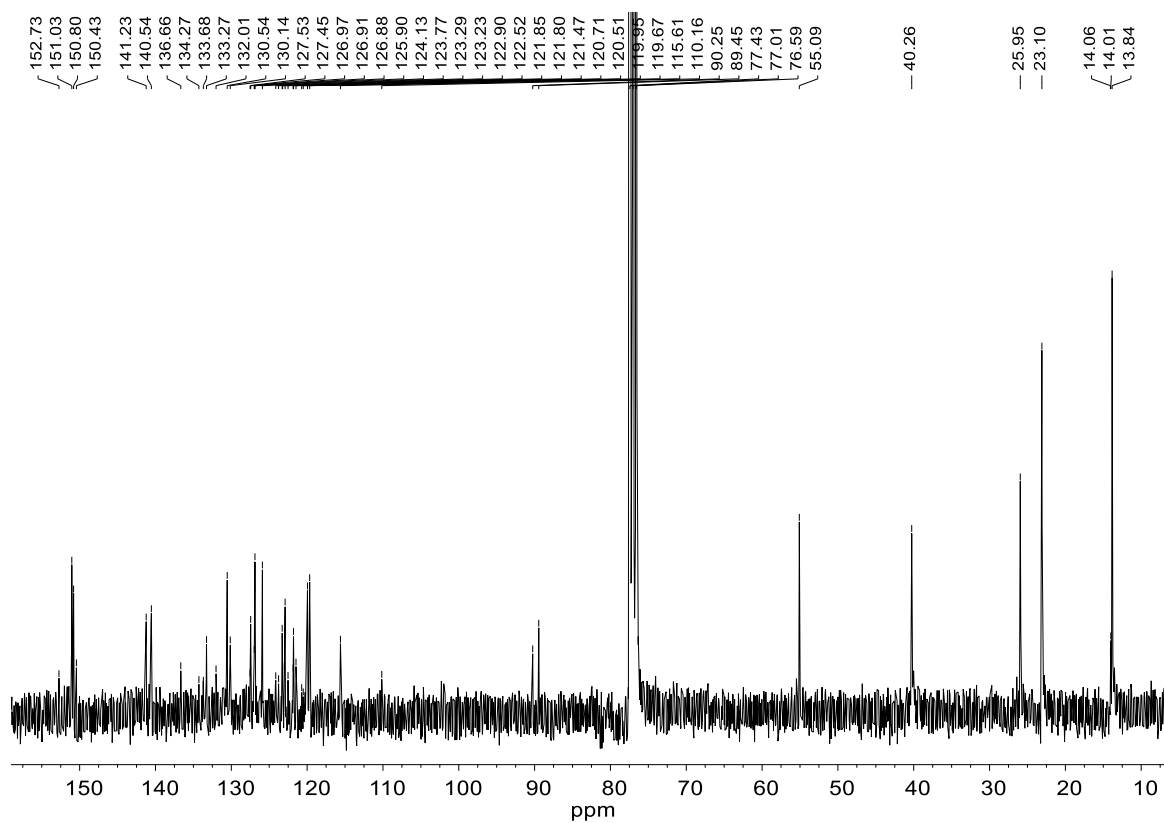## Porphyrin 7:

Porphyrin 8:
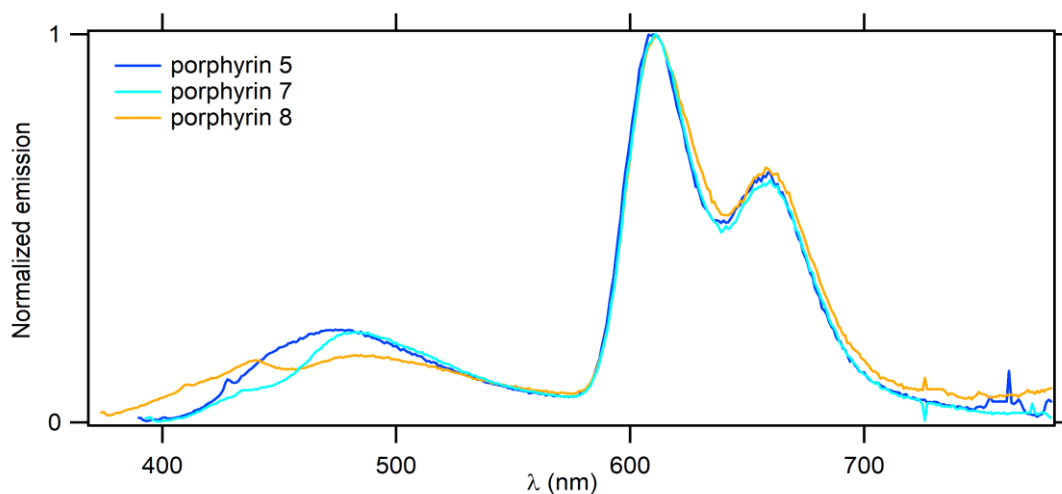
8. Energy transfer in porphyrins 1-8

Figure S16. Emission spectra upon UV excitation at the fluorenyl band for Zn(II) porphyrins **5**, **7** and **8**.

Derivation of Φ_{EnT} values. The energy transfer efficiency (Φ_{EnT}) from dendrons (D) towards the central porphyrin core (A) in porphyrins **1-4** and **5-8** was estimated based on the decrease in donor fluorescence in dichloromethane. It is given by:

$$\Phi_{EnT} = 1 - \Phi_{DA} / \Phi_D^0$$

where Φ_{DA} is the fluorescence quantum yield of the donor in the presence of the acceptor (*i.e.* the fluorescence quantum yield of the dendron in the presence of the porphyrin) and Φ_D^0 the fluorescence quantum yield of the donor in the absence of the acceptor *i.e.* the fluorescence quantum yield of the dendron model, in our case the aldehyde precursor (see Figure S16 for an example).

Table S1. Derivation of the energy transfer quantum yields in the free-base porphyrins **1-4** and in the Zn(II) complexes **6-8** using the corresponding aldehydes precursors **9-12** as models.[a]

Porphyrin	Donor model	Φ_{DA}	Φ_D^0	Φ_{EnT}
1	**9**	0.04	0.67	0.94
2	**10**	0.01	0.74	0.98
3	**11**	0.024	0.50	0.95
4	**12**	0.021	0.39	0.95
5	**9**	0.025	0.67	0.96
7	**11**	0.024	0.50	0.95
8	**12**	0.021	0.39	0.95

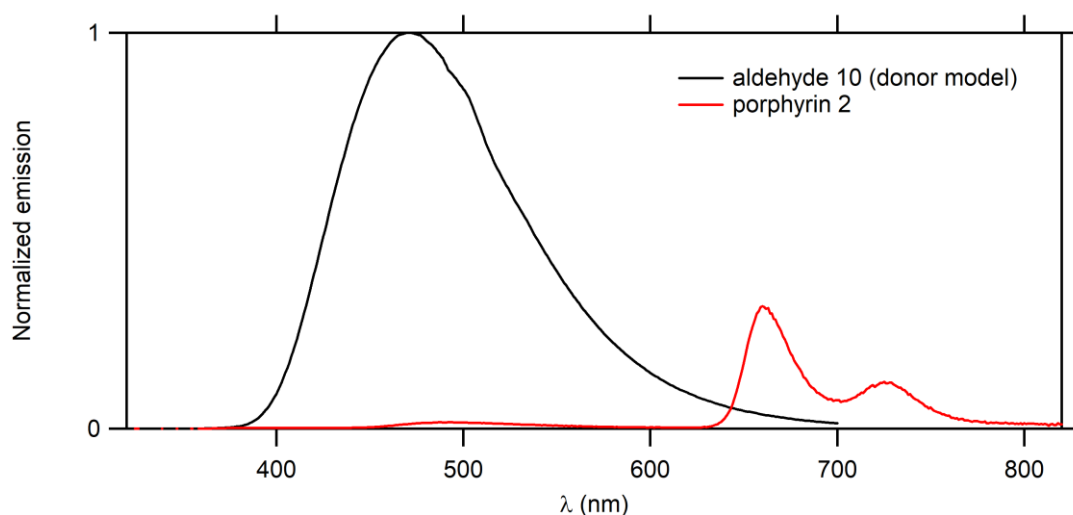[a] Fluorescence measurments done in CH_2Cl_2 solutions.

Figure S17. Example of fluorescence spectra of aldehyde **10** and porphyrin **2** (CH_2Cl_2) used for derivation of the energy transfer quantum yield.

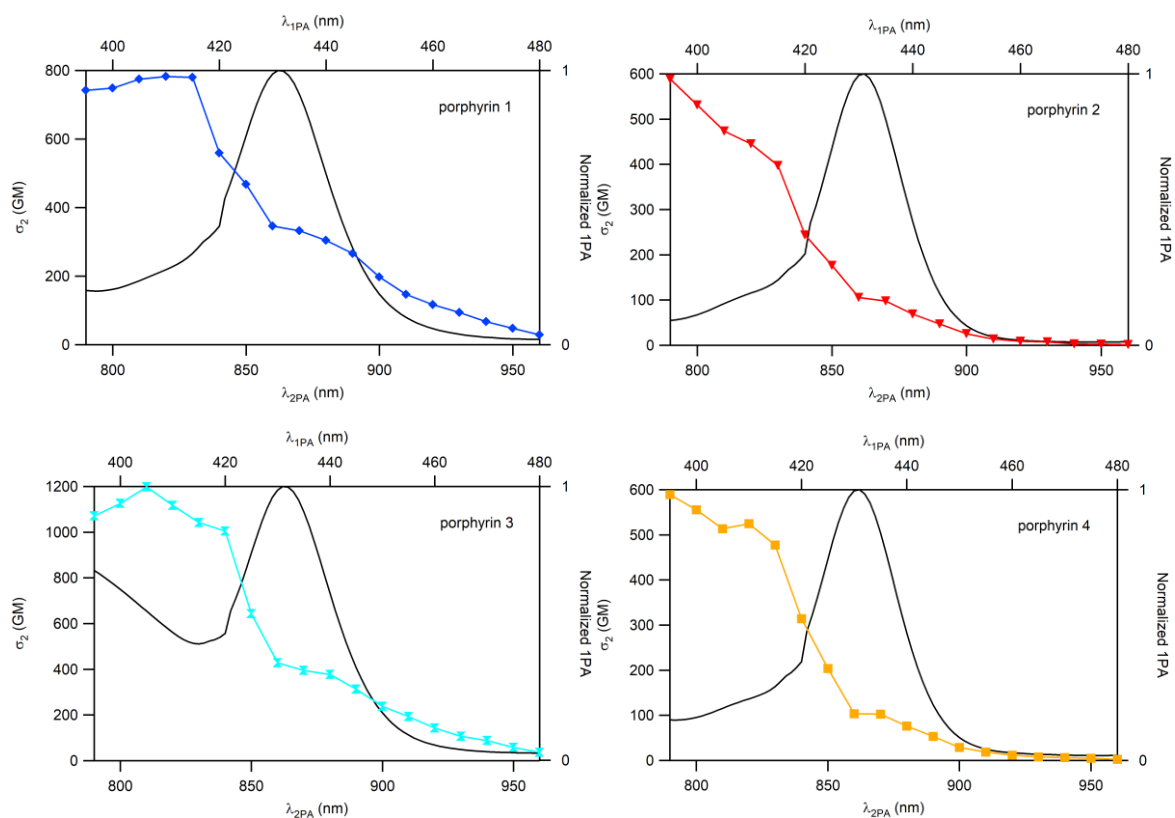## 9. Overlay of 1PA and 2PA spectra for selected compounds

Figure S18. Overlay of one- and two-photon absorption spectra for the free-base porphyrins **1-4** in CH_2Cl_2 (25 °C).
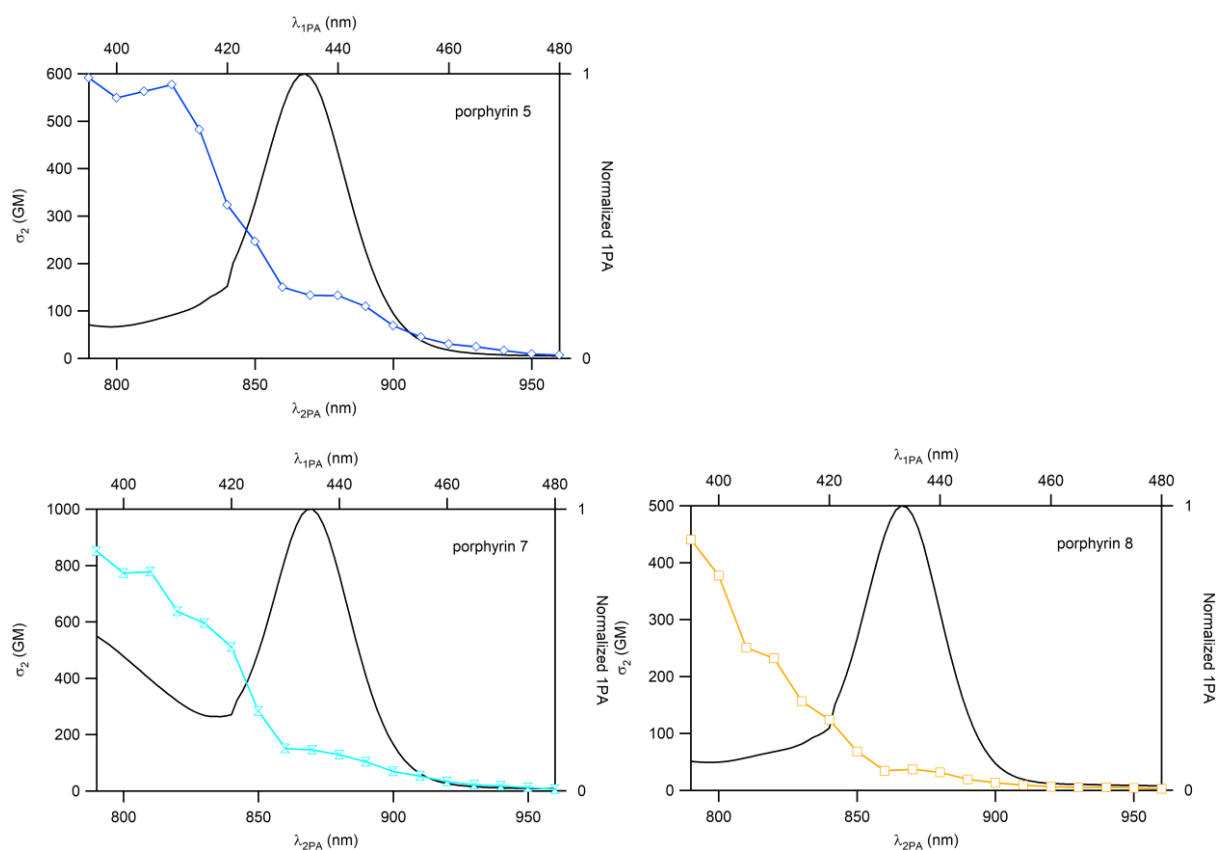
Figure S19. Overlay of one- and two-photon absorption spectra for the Zn(II) complexes **5**, **7-8** in CH$_2$Cl$_2$ (25 °C).
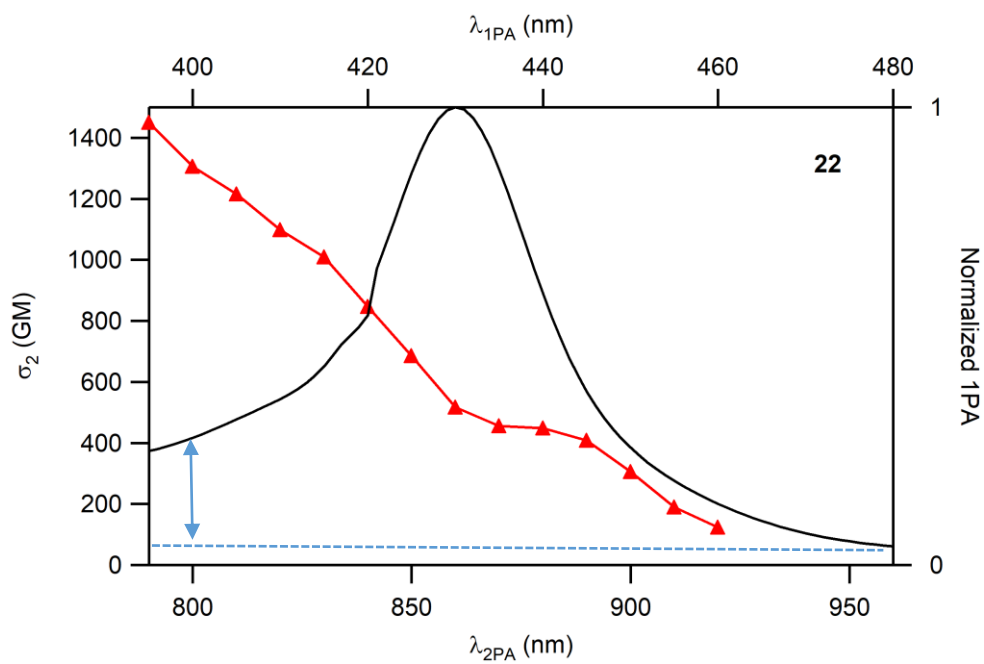

Figure S20. Overlay of one- and two-photon absorption spectra for the free-base porphyrin **22** in CH$_2$Cl$_2$. The overlap with the dendron-based band (peaking at higher energy) is revealed by the asymmetry of the Soret band.